Parametric Optimization of Electric Discharge Machining for AISI 1045 Steel: A Comprehensive Study

Optimización paramétrica del mecanizado por electroerosión para acero AISI 1045: un estudio exhaustivo

Otimização Paramétrica da Usinagem por Eletroerosão para Aço AISI 1045: Um Estudo Abrangente

Muhammad Mansoor Uz Zaman Siddiqui[1(*)], Syed Amir Iqbal[2], Ali Zulqarnain[3], Adeel Tabassum[4]

Recibido: 20/11/2024 Aceptado: 02/03/2025

Summary. - This study investigates the optimization of Electric Discharge Machining (EDM) parameters for AISI 1045. It is a medium carbon steel which is commonly used in automotive and aerospace industries because of its balanced strength, toughness and machinability. However, achieving optimal machining efficiency with excellent surface finish in short time and without wasting excess material with EDM remains a challenge at large. The research focuses on optimizing key EDM input parameters like current (LV), voltage (HV), pulse on time (Ton) and pulse off time (Toff), to improve machining time (Tm), material removal rate (MRR), electrode wear rate (EWR), surface roughness (Ra) and base radius (R). Full factorial design and Response Surface Methodology (RSM) were used to conduct experiments, and ANOVA was employed to identify the most significant factors influencing the output responses. Multi-objective optimization was performed through the desirability function and the findings were validated by repeated experiments. The results showed that pulse on time (Ton), its interaction with pulse off time (Toff) and the three-factor interaction between current (LV), Ton and Toff were the most significant factors affecting machining performance. Optimizing these parameters reduced machining time (Tm) to 623.21 seconds thus significantly improving EDM efficiency. The material removal rate (MRR) was maximized at 0.0173 g/min resulting in considerable increase in material removal efficiency. The electrode wear rate (EWR) was minimized to 0.0088 g/min, which prolongs electrode life and reduces operational costs. Surface roughness (Ra) was improved to 0.0253 mm, ensuring a high-quality surface finish. The base radius (R) was successfully optimized to 1.5298 mm, aligning closely with the desired target of 1.5 mm thus ensuring dimensional accuracy. This investigative study of optimization of parameters for EDM of AISI 1045 material is extremely significant for automotive and aerospace industries that rely on precision machining, as the optimized EDM parameters lead to improved efficiency, reduced material waste and enhanced product quality. These findings offer valuable insights for improving EDM processes, particularly in sectors requiring complex geometries and high precision, such as automotive and aerospace manufacturing.

Keywords: Electric Discharge Machining; AISI 1045; Parametric Optimization; Material Removal Rate; Electrode Wear Rate; Surface Roughness; Machining Time; Response Surface Methodology; ANOVA; Base Radius

Resumen. - *Este estudio investiga la optimización de los parámetros de mecanizado por descarga eléctrica (EDM) para AISI 1045. Es un acero de carbono medio que se utiliza comúnmente en las industrias automotriz y aeroespacial debido a su resistencia, tenacidad y maquinabilidad equilibradas. Sin embargo, lograr una eficiencia de mecanizado óptima con un excelente acabado superficial en poco tiempo y sin desperdiciar material sobrante con EDM sigue*

(*) Corresponding author.

[1] Master of Engineering, Department of Industrial Engineering, University of Engineering & Technology (Pakistan), 2023phdmnf1@student.uet.edu.pk,
ORCID iD: https://orcid.org/0009-0007-8992-7601

[2] Dean, Department of Industrial & Manufacturing Engineering, NEDUET (Pakistan), deanmme@neduet.edu.pk,
ORCID iD: https://orcid.org/0000-0002-6812-6238/

[3] Director Industrial Liaison, Department of Industrial & Manufacturing Engineering, NEDUET (Pakistan), dil@neduet.edu.pk,
ORCID iD: https://orcid.org/0000-0003-2762-5409

[4] Mechanical Engineer, Department of Mechanical Engineering, NUST (Pakistan), adeeltabassum1@gmail.com,
ORCID iD: https://orcid.org/0009-0006-9375-1090

Memoria Investigaciones en Ingeniería, núm. 28 (2025). pp. 222-268
https://doi.org/10.36561/ING.28.15
ISSN 2301-1092 • ISSN (en línea) 2301-1106 – Universidad de Montevideo, Uruguay

siendo un desafío en general. La investigación se centra en la optimización de los parámetros de entrada clave de EDM como la corriente (LV), el voltaje (HV), el tiempo de activación del pulso (Ton) y el tiempo de desactivación del pulso (Toff), para mejorar el tiempo de mecanizado (Tm), la tasa de remoción de material (MRR), la tasa de desgaste del electrodo (EWR), la rugosidad superficial (Ra) y el radio base (R). Se utilizaron el diseño factorial completo y la Metodología de Superficie de Respuesta (RSM) para realizar experimentos y se empleó ANOVA para identificar los factores más significativos que influyen en las respuestas de salida. Se realizó una optimización multiobjetivo a través de la función de deseabilidad y los hallazgos se validaron mediante experimentos repetidos. Los resultados mostraron que el tiempo de activación del pulso (Ton), su interacción con el tiempo de desactivación del pulso (Toff) y la interacción de tres factores entre la corriente (LV), Ton y Toff fueron los factores más significativos que afectaron el rendimiento del mecanizado. La optimización de estos parámetros redujo el tiempo de mecanizado (Tm) a 623,21 segundos, mejorando así significativamente la eficiencia de la electroerosión. La tasa de eliminación de material (MRR) se maximizó a 0,0173 g/min, lo que resultó en un aumento considerable en la eficiencia de eliminación de material. La tasa de desgaste del electrodo (EWR) se minimizó a 0,0088 g/min, lo que prolonga la vida útil del electrodo y reduce los costos operativos. La rugosidad superficial (Ra) se mejoró a 0,0253 mm, lo que garantiza un acabado superficial de alta calidad. El radio base (R) se optimizó con éxito a 1,5298 mm, alineándose estrechamente con el objetivo deseado de 1,5 mm, lo que garantiza la precisión dimensional. Este estudio de investigación sobre la optimización de parámetros para la electroerosión de material AISI 1045 es fundamental para las industrias automotriz y aeroespacial que dependen del mecanizado de precisión, ya que la optimización de los parámetros de la electroerosión mejora la eficiencia, reduce el desperdicio de material y mejora la calidad del producto. Estos hallazgos ofrecen información valiosa para mejorar los procesos de electroerosión, especialmente en sectores que requieren geometrías complejas y alta precisión, como la fabricación automotriz y aeroespacial.

Palabras clave: *Mecanizado por electroerosión; AISI 1045; Optimización paramétrica; Tasa de remoción de material; Tasa de desgaste de electrodos; Rugosidad superficial; Tiempo de mecanizado; Metodología de superficie de respuesta; ANOVA; Radio base*

Resumo. - *Este estudo investiga a otimização dos parâmetros de usinagem por descarga elétrica (EDM) para AISI 1045. É um aço de médio carbono comumente usado nas indústrias automotiva e aeroespacial devido à sua resistência, tenacidade e usinabilidade equilibradas. No entanto, atingir a eficiência de usinagem ideal com excelente acabamento superficial em curto espaço de tempo e sem desperdiçar excesso de material com EDM continua sendo um grande desafio. A pesquisa se concentra na otimização dos principais parâmetros de entrada de EDM, como corrente (LV), tensão (HV), tempo de pulso ligado (Ton) e tempo de pulso desligado (Toff), para melhorar o tempo de usinagem (Tm), taxa de remoção de material (MRR), taxa de desgaste do eletrodo (EWR), rugosidade da superfície (Ra) e raio da base (R). O planejamento fatorial completo e a Metodologia de Superfície de Resposta (RSM) foram usados para conduzir experimentos e ANOVA foi empregada para identificar os fatores mais significativos que influenciam as respostas de saída. A otimização multiobjetivo foi realizada por meio da função de desejabilidade e os resultados foram validados por experimentos repetidos. Os resultados mostraram que o tempo de pulso ligado (Ton), sua interação com o tempo de pulso desligado (Toff) e a interação de três fatores entre corrente (LV), Ton e Toff foram os fatores mais significativos que afetaram o desempenho da usinagem. A otimização desses parâmetros reduziu o tempo de usinagem (Tm) para 623,21 segundos, melhorando significativamente a eficiência da EDM. A taxa de remoção de material (MRR) foi maximizada em 0,0173 g/min, resultando em um aumento considerável na eficiência da remoção de material. A taxa de desgaste do eletrodo (EWR) foi minimizada para 0,0088 g/min, o que prolonga a vida útil do eletrodo e reduz os custos operacionais. A rugosidade da superfície (Ra) foi melhorada para 0,0253 mm, garantindo um acabamento superficial de alta qualidade. O raio da base (R) foi otimizado com sucesso para 1,5298 mm, alinhando-se estreitamente com o alvo desejado de 1,5 mm, garantindo assim a precisão dimensional. Este estudo investigativo sobre a otimização de parâmetros para eletroerosão do material AISI 1045 é extremamente significativo para as indústrias automotiva e aeroespacial que dependem de usinagem de precisão, visto que os parâmetros otimizados de eletroerosão levam a uma maior eficiência, redução do desperdício de material e melhoria da qualidade do produto. Essas descobertas oferecem insights valiosos para o aprimoramento dos processos de eletroerosão, particularmente em setores que exigem geometrias complexas e alta precisão, como a indústria automotiva e aeroespacial.*

Palavras-chave: *Usinagem por Descarga Elétrica; AISI 1045; Otimização Paramétrica; Taxa de Remoção de Material; Taxa de Desgaste do Eletrodo; Rugosidade da Superfície; Tempo de Usinagem; Metodologia de Superfície de Resposta; ANOVA; Raio da Base.*

1. Introduction. - The machining techniques that are generally used in the industry can be categorized into conventional and non-conventional methods. The conventional machining process removes material from a workpiece using mechanical techniques such as cutting, shearing, and abrasion. The techniques used can be milling, grinding, drilling and turning (1). When the conventional machining techniques are applied, hard tools are used to shape the workpiece to the required size and surface finish. Conversely, the non-conventional machining methods use alternative techniques that are dependent on sources of high energy or other methods that can support in removal of material from the workpiece. These methods include water jet machining (2), ultrasonic machining (3) (4), laser cutting (5) (6), electrical discharge machining (EDM) (7) (8) and electrochemical machining (9) (10). The common applications for the non-conventional machining processes are hard materials, complex geometries and those areas where the conventional processes lose their effect. The parts produced are relatively accurate machined flexibly when these techniques are utilized.

There's always a need for usage of versatile materials that can be used for a wide range of applications in which the material should show a balance between toughness, strength and wear resistance. Electric Discharge Machining (EDM) is particularly well-suited for machining AISI 1045 due to its ability to handle hard materials and complex geometries without inducing mechanical stress. AISI 1045 is a medium carbon steel with a moderate carbon content (0.43-0.5%) and is widely used in industries requiring high strength and wear resistance, such as automotive and aerospace. However, its hardness makes it challenging to machine using conventional methods, especially for intricate shapes and tight tolerances. EDM is a contact less process and uses electrical impulses to erode material, making it ideal for such applications. Additionally, EDM provides excellent surface finish quality, reducing the need for post-processing steps like polishing or grinding. These advantages make EDM the preferred choice for machining AISI 1045 in precision-critical applications.

Electrical Discharge Machining (EDM) is particularly well-suited for machining AISI 1045 due to the material's properties and the unique capabilities of the EDM process. AISI 1045, a medium-carbon steel, is known for its good tensile strength and wear resistance, making it a popular choice for components such as gears, shafts, and machinery parts. However, its hardness and toughness can pose challenges for conventional machining methods, especially when intricate shapes or fine surface finishes are required. EDM, being a non-contact machining process that uses electrical discharges to remove material, is ideal for such scenarios. It can efficiently machine hard materials like AISI 1045 without inducing mechanical stress or tool wear, which are common issues in traditional machining. This makes EDM a preferred method for achieving precise geometries and high-quality surface finishes on AISI 1045 components.

There are several industrial applications of AISI 1045 material which includes construction usage, tool and die making, automotives industry and agriculture. In industrial applications, this material is used to make shafts, gears and couplings, bolts and studs, crankshafts and connecting rods etc. In construction applications, its usage comes for those structural components where a balance between strength and toughness is the task. In the dies and tools where wear resistance and medium strength is required, this material is utilized. In automotive industry, this material is used to manufacture axles as well as engine components (11). Similarly, it is used to produce components which are assembled in agricultural machinery. This material has also found its way in the nuclear industry (12).

In EDM process, the manufacturing is carried out via electric discharge to obtain the desired shape. It works on the workpiece as the material is eroded thermally. For usage of EDM on AISI 1045, it is preferable in some circumstances which encompass a number of factors. The need for EDM on this material arises when the geometries are complex as EDM is capable of producing intricate shapes with fine details that are not possible with conventional methods. Also, when thin walls and sharp corners are required, EDM supports prevention of deformation in the components. AISI 1045 is good at heat treatment hardening as it becomes wear resistant at the same time it's a challenge to machine it uses conventional cutting processes (13). EDM is capable to machine this material with minimal tool wear. EDM on AISI 1045 is also needed when there are tight tolerances and high precision to produce exact dimensions in critical parts. After optimizing the input parameters and output responses, this manufacturing procedure reduces the need for final processing steps like polishing or grinding. Since EDM is a non-contact process, deflection of tool and wearing can be eliminated as it happens when processing hard materials conventionally. EDM also has better accessibility and reaches internal cavities where conventional machining process doesn't support.

The advantages of using EDM on AISI 1045 are quite impressive. There isn't any mechanical stress as there isn't any type of direct contact between the electrode and workpiece as EDM is capable to machine hard materials with high accuracy and precision with excellent surface finish due to which multiple and additional process requirements as in non-conventional machining are eliminated (14). The application of EDM on AISI 1045 includes die and mold making for injection molding as well as metal forming and stamping (15). Its's application in tool and die industry for customized jigs and fixtures preparation is also noticeable (16). It is also used for rapid prototyping where complex geometries are required. It can also be utilized in preparation of surgical instruments and medical implants in medical devices (17). Most importantly, in automotive and aerospace industry, AISI 1045 is the choice for intricate parts manufacturing for engines and also precision components (18).

EDM process has its own set of limitations which are an area of interest for researchers (19). EDM usually has a slower rate when it comes to material removal i.e. MRR thus resulting in higher machining times (Tm). The conventional processes are much faster in terms of material removal rate. Secondly, the initial setup cost of EDM is much higher as compared to conventional subtractive manufacturing techniques. Material should also be electrically conductive in order to be used for EDM. On reviewing the literature, it came to the authors' knowledge that a very limited work has been carried out on AISI 1045 when it comes to die sinking EDM process as most of the research work is carried out with wire EDM (20) or conventional machining processes (21). Haron et al had performed experiment with varying copper electrode diameter (9.5, 12 and 20 mm) and current value (3.5 and 6.5 A) to determine the optimum value of material removal rate (MRR) and electrode wear rate (EWR) (22). Kumar and Agarwal had performed machining parameters optimization for surface roughness in the EDM processing of AISI 1045 (23). There seemed a need to carry out a comprehensive study to determine the effect of various input parameters including current (LV), voltage (HV), pulse on time (Ton) and pulse off time (Toff) and monitor the various output parameters including MRR, EW, machining time (Tm), base radius (R) and machined surface roughness (Ra) and optimize them accordingly. For large scale manufacturers and designers, all output responses like Machining time (Tm), material removal rate (MRR), electrode wear rate (EWR), surface roughness (Ra), base radius (R) are of extreme importance and compromise on any of the responses means major loss in productivity or product quality. Currently there is no single study present at this point of time where the afore mentioned parameters and their output responses have been considered in totality when the EDM process of AISI 1045 is considered (24) (8) (25) (20) (26). This is of great importance for manufacturers in automotive engine manufacturing, dies and mold makers, aerospace industry, bio medical machine manufacturing etc. The current experimental research for optimizing the parameters was carried out in a meticulous setting and results of the study were positive.

2. Materials and methods. -

2.1 Materials. - AISI-1045 is a low-cost alloy suitable for most engineering and construction applications. It is a medium carbon steel with adequate strength and toughness characteristics and is valuable for induction or flame hardened components and can provide a typical surface hardness of up to 58 HRC. The typical applications include construction applications, bolts, axles, connecting rods, pins, rams, studs spindles, ratchets etc.

The authors have used copper electrode as it is a good performer in surface finishing and quality compared to graphite. When using a graphite electrode, increased tool wear and poor surface quality are observed (27). The dielectric used in the experiment is kerosene oil. K., Masoud Pour & S. Ehsan Layegh (2022) have conducted a study to optimize MRR, Ra and surface topography on tool steels including AISI 1045 under the influence of ZnO nanoparticles. The study concluded that the optimized values for input factors AISI 1045 had been achieved using 2 g of the ZnO nanoparticles that had reduced the Ra by 16.66% (18).

In the current research, the experimentation has been carried out in a controlled environment with lower levels of input factors, these resulted in positive output. The results will be discussed in detail in the results section.

The chemical composition of AISI-1045 is listed in Table

Element	**%**
Carbon (C)	0.45
Manganese (Mn)	0.75
Silicon (Si)	0.25
Sulphur (S)	0.05 max.
Phosphorous (P)	0.05 max.
Iron (Fe)	Balance

Table I. Chemical Composition of AISI 1045.

When transistorized, pulse-type power supplies, either electrolytic or pure were developed, the metallic electrode that became preferable was copper as copper along with specific levels of power supply supports in low burning due to wear. If graphite is consumed in the same setting, the tool wear is high. Moreover, for advanced power supply circuits with polishing performed, copper is compatible. Copper produces a good surface finish due to its structural integrity compared to the counterpart graphite. This property further resists DC arcing where flushing is poor. On a wire EDM, Female electrodes are commonly utilized in copper for usage in reverse burning punches and cores in the sinker EDM (25) (26).

2.2 Methods. - In this study, the researchers had planned the experiments to optimize the output responses like machining time (Tm), material removal rate (MRR), electrode wear rate (EWR), surface roughness (Ra) and base radius (R) using design of experiments (DOE) and Response Surface Methodology (RSM).

2.2.1 Design of experiments (DOE). - Planning any data collection activities in the face of variability, whether or not the experimenter has complete control, is known as design of experiments (DOE). It entails a group of tests or a sequence of tests in which the input variables of a system or process are purposefully changed. The goal is to methodically monitor and pinpoint the reasons for variations in the output responses (28).

2.2.2 Response Surface Methodology (RSM). - It is a statistical and mathematical method for optimizing processes and determining the correlations between numerous input factors and one or more output replies. It is especially effective for modeling and analyzing issues whose outcomes are influenced by multiple variables. RSM combines experimental design, regression analysis and optimization approach to create a mathematical model (usually a second-order polynomial) that predicts response behavior based on input elements. The method aids in determining ideal conditions for processes and is frequently used in engineering, manufacturing and other sectors to increase efficiency, product quality and performance.

3. Experimental Methodology. - The experimental design was based on the Design of Experiment (DOE) technique, especially a full factorial design. This method enables a thorough examination of the essential effects and interactions among the four selected input parameters: pulse on time (Ton), pulse off time (Toff), current (LV) and voltage (HV). Each of these parameters was examined at two different levels, high and low, allowing for a thorough examination of their effect on output responses. Values of the input parameters are mentioned in the Table .

Factor	Levels	No. of Levels
Workpiece	AISI 1045	1
Pulse on time (T_{on})	4 µs, 6.5µs	2
Pulse off time (T_{off})	5.5 µs, 6.5 µs	2
Current (LV)	30 A, 50 A	2
Voltage (HV)	0.3 V, 0.7 V	2

Table II. Values of input parameters along with levels.

Pulse on time (Ton) was chosen because it directly affects the energy delivered to the workpiece during each pulse. Longer pulse durations result in higher energy input consequently resulting in increased material removal rate but this can also lead to higher electrode wear and surface roughness. In order to optimize all the output lower Ton values (4 µs and 6.5 µs) were selected to minimize electrode wear and reduce excessive heat generation, which is crucial for precision applications. Similarly, pulse off time (Toff) was included because it controls the cooling time between pulses. A slightly higher Toff (5.5 µs and 6.5 µs) was chosen to enhance flushing efficiency, ensuring better debris removal and maintaining process stability. This helps prevent short circuits and improves surface finish. The study avoided very low Toff values, as they could lead to insufficient cooling and debris removal, causing instability in the machining process.

Current (LV) was another critical parameter selected for optimization because it influences the intensity of the electrical discharge. The study chose current levels of 30 A and 50 A to balance power consumption and material removal efficiency. Lower currents (30 A) are more energy-efficient and suitable for fine machining, while higher currents (50 A) increase MRR but may also increase electrode wear and surface roughness. Very high currents were avoided because they could lead to excessive electrode wear and thermal damage, while very low currents might result in insufficient material removal, making the process inefficient. Voltage (HV) was also included because it affects the spark gap and the energy of each discharge. The study selected lower voltage levels (0.3 V and 0.7 V) to reduce thermal damage and improve surface finish. Lower voltages are more suitable for precision machining, as they help achieve finer surface finishes and tighter tolerances. Higher voltages were not considered because they could lead to larger craters on the workpiece surface, increasing surface roughness and reducing dimensional accuracy.

Other parameters, such as electrode material and dielectric fluid, were kept constant to isolate the effects of the primary electrical parameters under investigation. Copper electrodes were chosen because they are known for their good surface finish and lower wear rates compared to graphite electrodes, which tend to produce poorer surface quality and are less suitable for precision applications. Kerosene was selected as the dielectric fluid due to its effectiveness in flushing debris and cooling the workpiece and electrode. Other dielectric fluids, such as deionized water or oil-based fluids, were not considered because kerosene is widely used in EDM processes and provides a good balance between cost and performance. The duty factor, which is the ratio of Ton to the total cycle time, was indirectly controlled by the selection of Ton and Toff. The study did not explicitly vary the duty factor as a separate parameter because it is linked to Ton and Toff. The chosen Ton and Toff values already provided a reasonable range of duty factors (38% to 54%), which were sufficient to study the effects on machining performance. Parameters such as flushing pressure was not varied in this study. Flushing pressure is crucial for debris removal. It was kept constant because the focus was on optimizing electrical parameters rather than mechanical factors. The study assumed a constant flushing pressure that was sufficient to maintain process stability.

Based on these input parameters, basic experimental runs were performed and data of output responses against input factors were recorded. These basic experimental runs are mentioned in Table III. Basic experimental runs for AISI-1045 on Table .

3.1 Workpiece preparation. - The workpieces (Figure) used in these experiments consisted of two grounded blocks, each with dimensions of 100 x 10 x 20 mm, secured in place using dowel pins. Electrode is of copper material (Figure). Dielectric is of kerosene + C10 material.

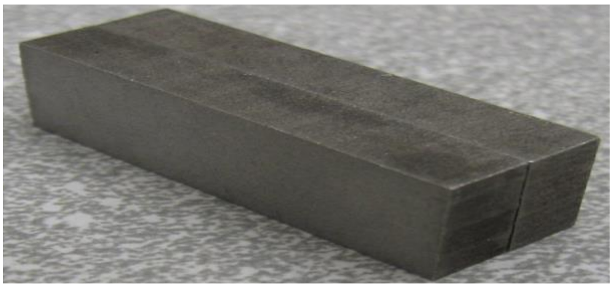

Figure I. Parted Workpiece Snapshot before Machining.

Figure II. Copper Electrode Tip at 17 X prior to Machining.

3.2 Equipment used:

- EDM machine = Genspark E5B1041
- Weighing scale = AND GF-200 with least count of 0.001 g
- Surface roughness tester = Wilson Wolpert CM T2
- Microscope = Stereo microscope with 45X magnification with CMOS chip

EDM machine is available in Figure , weighing scale in Figure , surface roughness tester in Figure and microscope in Figure .

Figure III. Genspark E5B1041.

Figure IV. Precision weighing scale AND GF-200.

Figure V. Surface Roughness Tester WW CM T2.

Figure VI. Stereo microscope.

EWR was calculated using the equation mentioned below in Equation 1:

$$EWR = \frac{Eb - Ea}{Tm}\ (g/\text{min})$$

Equation 1 Equation to calculate electrode wear rate

MRR was calculated using the equation mentioned below in Equation 2:

$$MRR = \frac{Wb - Wa}{Tm}\ (g/\text{min})$$

Equation 2 Equation to calculate material removal rate

3.3 Objectives. - The objectives of this experimental study are as follows:
1. To reduce the machining time (Tm) for AISI 1045 steel via the EDM technique.
2. To improve the material removal rate (MRR) during EDM machining of AISI 1045 steel.
3. To reduce the electrode wear rate (EWR) when treating AISI 1045 steel using EDM.
4. To improve surface roughness (Ra) on AISI 1045 steel with EDM.
5. Minimize variations in the base radius (R) of AISI 1045 steel machined with EDM.

3.4 Analysis of Variance (ANOVA). - The experimental data that was performed on the basis of basic experimental runs as mentioned in Table was examined by using statistical techniques and conclusions were drawn based on the significance of the components and their interactions. A 95% confidence interval was used and factors with the p-values less than 0.05 were considered as significant. The normal plot of standardized effects was used to distinguish between significant and non-significant components, whilst residual plots evaluated the model's fit. After that the model was then refitted by removing the non-significant factors and a revised ANOVA table was created. Now this revised ANOVA table consists of only significant factors and all non-significant factors are eliminated in order to better understand the impact of input factors on output responses. Main effect plot and interaction plots were also created. A high slope in the main effects plot showed significant factors, while non-parallel lines in the interaction plot indicated significant relationships at the factor level. The Response Optimizer tool was used to perform optimization, with targets such as response minimization, maximization or equating established. The desirability function was studied by specifying lower, target and upper bounds, with a desirability (d) value near to 1 indicating that the response is close to the target. The results (Table and Table) produced optimal values for the major factors, their response values and the desirability factor. The findings were validated by replicating the studies and the optimal solutions were put into practice. Detailed experimental results and replicates are available in Appendix 7 and Appendix 8.

4. Results and Discussion. -

4.1 Experimental results and analysis. -

4.1.1 Optimized results for machining time (Tm). - The machining time (Tm) for AISI 1045 was optimized using ANOVA in Minitab in which all the input factors were considered and their interaction with output responses were calculated to determine significant causes to the variation in machining time. The purpose of this investigation was to reduce machining time thereby increasing the efficiency of the EDM process. All detailed graphs and table are present in Appendix 2. Machining pictures of electrode and workpiece are given in Appendix 9 and Appendix 10.

Initially all input parameters like pulse on time (Ton), pulse off time (Toff), current (LV) and voltage (HV) were considered along with their interactions with output response of machining time. Significant factors were identified using p-value and a 0.05 threshold for significance was considered. The p-value is used to determine the statistical significance of each input factor and their interactions. A p-value less than 0.05 indicates that the factor or interaction has a significant effect on the machining time (Tm). The ANOVA Table and normal probability plots (Figure and Figure) and residual plots (Figure and Figure) showed that the input factor i.e. pulse on time (Ton), interaction between pulse on time (Ton) and pulse off time (Toff) (Ton*Toff) and the three-factor interaction between LV, Ton and Toff (LV*Ton*Toff) were statistically significant in terms of their influence on the output response which is machining time. These significant input factors p-values are listed below (Table):

- Ton = 0.000
- Ton*Toff = 0.021
- LV*Ton*Toff = 0.024

The interaction between Ton and Toff is significant because it represents the balance between energy input and cooling time. Longer Ton increases the energy delivered per pulse, leading to higher material removal rates (MRR), but it also generates more heat, which can increase electrode wear and surface roughness. Toff, on the other hand, provides time for cooling and debris removal. The study found that specific combinations of Ton and Toff can optimize MRR while minimizing electrode wear and surface roughness. For example, a longer Ton combined with a slightly longer Toff can enhance material removal efficiency without causing excessive heat buildup or debris accumulation. This interaction highlights the need to carefully balance energy input and cooling to achieve optimal machining performance.

This three-factor interaction is significant because it reflects the combined effect of current, pulse duration, and cooling time on machining performance. Higher current (LV) increases the intensity of the electrical discharge, leading to higher MRR, but it also increases electrode wear and surface roughness. When combined with longer Ton, the energy input is further amplified, which can lead to excessive material removal and thermal damage if not balanced with an appropriate Toff. The study found that optimizing this three-factor interaction can significantly reduce machining time

(Tm) while maintaining acceptable levels of electrode wear and surface finish. For instance, a higher current combined with longer Ton and a slightly longer Toff can maximize material removal efficiency while ensuring sufficient cooling and debris removal. This interaction underscores the importance of coordinating current, pulse duration, and cooling time to achieve a balance between productivity and quality.

The model was then refitted by eliminating non-significant factors as mentioned in Table . The revised model in main effect plot (Figure) and residual plot (Figure) showed that both the model and the major factors Ton, Ton*Toff and LV*Ton*Toff were still significant.

For machining time optimization, the target value was set to '0', while the upper bound value was set at 343 seconds, which reflected the shortest observed machining time during the experiment. The desirability function in Figure was used to calculate the optimized values of the machining time. The desirability function's target was set at '0' for machining time to minimize processing duration, as shorter machining times are desirable for industrial efficiency. The resulting desirability value (d = 0) suggested that the response (Tm) was far from the target value, implying that the target of '0' was unsuitable for this particular response. The response was much below the highest limit (343 seconds), resulting in a lower desirability. If the target had been set closer to 600 seconds with a larger upper bound (e.g., 1000 seconds), the desirability would have approached one, indicating a greater alignment with the optimization goal.

For the optimized value of output response of Tm, following values of input factors came out to be significant where lowest machining time was achieved.
Current (LV) = 30 A; Pulse on time (Ton) = 6.5 µs and pulse off time (Toff) = 5.0 µs.
The minimal machining time for these optimized parameters was found to be 623.2083 seconds.

Significant input factors that were calculated for output response of machining time shows both direct and inverse relation Tm. Pulse on time (Ton) was found to be directly proportional to Tm and this shows that as Ton will increase machining time will also increase which is understandable as longer Ton increases the energy input each for pulse thus increasing the machining time. On the other hand, the interaction between Ton and pulse off time (Toff) (Ton*Toff) showed a complex relationship because certain combinations of these two parameters resulted in shorter machining times. Furthermore, the three-factor interaction (LV*Ton*Toff) showed that when current is considered along with pulse on and off times overall machining time will reduce because more material will be removed from workpiece surface as current is higher along with increased pulse duration. These interactions show that the Tm is highly sensitive to both individual factors and their interactions and this suggests that the input parameters interactions must be carefully adjusted to get the best and optimized results.

4.1.2 Optimized results for material removal rate (MRR). - The optimization of material removal rate (MRR) for AISI 1045 was carried out using ANOVA in Minitab. All input factors, including pulse on time (Ton), pulse off time (Toff), current (LV) and voltage (HV) were considered with the goal of maximizing MRR. Significant factors were identified by examining the p-values in the ANOVA table, with a significance threshold of 0.05. All tables and figures are present in Appendix 3.

From the ANOVA Table and the normal probability plot (Figure and Figure) and residual plot (Figure and Figure), Ton and the interaction between Ton and Toff (Ton*Toff) were considered to be significant factors that are affecting MRR. The p-values of significant factors are listed below (Table):

- Ton = 0.000
- Ton*Toff = 0.034

Following this, the model was refitted by excluding non-significant factors and focusing only on Ton and Ton*Toff interaction as mentioned in Table .

Now the main effects plot in Figure and interaction plot in Figure for MRR were prepared. The main effects plot showed a steep slope for means showing the importance of Ton and Ton*Toff. Additionally, the interaction plot revealed non-parallel lines, highlighting the significant interaction between Ton and Toff in calculating MRR.

The desirability function is a widely used approach in multi-objective optimization to convert multiple response variables into a single composite desirability score, ranging from 0 (least desirable) to 1 (most desirable). In the optimization of Material Removal Rate (MRR) for EDM machining of AISI 1045, the desirability function was employed to determine the best combination of pulse on time (Ton) and pulse off time (Toff) that maximizes MRR while ensuring process stability and efficiency. For the optimization of MRR, the target value was set to '1', while the lower bound was set at 0.0304 g/min, which represented the maximum observed MRR during the experiment. The desirability function (Figure) was used to assess how closely the optimized values aligned with the target. A desirability value of d = 0 indicated that the response (MRR) was far from the set target of '1', suggesting that this target was unrealistic for the given response. The response was much lower than the upper limit (0.0304 g/min), resulting in a lower desirability. Had the target been set closer to 0.02 g/min with a lower upper limit (e.g., 0.001 g/min), the desirability would have approached one, indicating better alignment with the optimization objective.

The optimization process resulted in the following significant input factor values for maximizing MRR:

- Ton (Pulse on time): 6.5 µs
- Toff (Pulse off time): 5.5 µs

On these optimized settings, the maximum MRR achieved was 0.0173 g/min, which reflects the optimized material removal under the given experimental conditions. This optimization highlights the critical influence of both Ton and its interaction with Toff on the material removal rate during EDM machining of AISI 1045 steel.

Ton and MRR are directly proportional to each other because higher energy cycle will lead to more material removed from the workpiece leading to higher MRR. While on the other hand interaction between Ton and Toff is complex in nature. As Ton increased material removal rate, optimal time is needed so that the workpiece temperature of that particular section cools down but not completely solidified between pulses ensuring efficient material removal.

4.1.3 Optimized results for electrode wear rate (EWR). - The analysis of Electrode Wear Rate (EWR) for AISI 1045 was carried out using ANOVA in Minitab. All input factors were considered including pulse on time (Ton), pulse off time (Toff), current (LV) and voltage (HV). The objective of this analysis was to minimize the EWR thereby increasing electrode life and improving overall machining efficiency. Significant factors affecting EWR were identified by evaluating the p-values from the ANOVA table, with a threshold of 0.05 indicating statistical significance. All detailed graphs and table are present in Appendix 4.

ANOVA Table , normal probability plot (Figure) and residual plot (Figure and Figure) showed that Ton was the only significant factor affecting EWR and its p-value was 0.001 (Table). Now the model was refitted by excluding all the non-significant factors and only Ton as the primary influencing variable. The p-values in the revised ANOVA Table confirmed that the refitted model, as well as the factor Ton, were statistically significant in determining the variation in EWR.

Now the main effects plot (Figure) and interaction plot (Figure) were prepared for EWR. The main effects plot showed a steep slope thus confirming the significance of Ton in influencing EWR. The interaction plot further showed non-parallel lines meaning that interactions among other factors did not contribute significantly to EWR. This established the fact that Ton as the key variable in this analysis.

For optimization of EWR, the target value was set to '0', while the upper bound value was established at 0.00551 g/min, which represented the minimum observed EWR in the experiments. The desirability function (Figure) was utilized to determine how closely the optimized values aligned with the desired target. A desirability value of d = 0 showed that the response (EWR) was far from the set target of '0', highlighting that this target was not practically attainable for this specific response. The actual EWR was much below the upper bound, resulting in a lower desirability score. If the target had been set closer to 0.009 g/min and the upper bound set to a larger value (e.g., 0.01 g/min), the desirability would have approached one, signaling better alignment with the optimization goal.

Through the optimization process, the significant input factor (Ton) was determined to have the following optimized value for minimizing EWR:

- Pulse on time (Ton) = 4.0 µs

With this optimized Ton value, the minimum EWR was calculated to be 0.0088 g/min, reflecting the ideal electrode wear rate achievable under these experimental conditions. This optimization highlights the critical role of Ton in controlling electrode wear, as shorter pulse durations reduce electrode erosion, lowering the wear rate during EDM machining of AISI 1045 steel. Optimized results for surface roughness (Ra)

The surface roughness (Ra) for AISI 1045 was analyzed using ANOVA in Minitab. The goal was to minimize the surface roughness, thus improving the surface quality of the workpiece. All input factors, including voltage (HV), pulse on time (Ton), pulse off time (Toff) and current (LV) were initially considered to identify significant input factors that can have possible impact on the output response i.e. surface roughness. The analysis was conducted by assessing p-values from the ANOVA table, with a significance threshold set at 0.05. All detailed graphs and table are present in Appendix 5.

ANOVA table (Table), normal probability plot (Figure and Figure) and residual plot (Figure and Figure) showed that the three-way interaction between HV, Ton and Toff (HV*Ton*Toff) was a significant factor affecting surface roughness (Ra) and its p-value came out to be 0.039 (Table). Now the model was refitted (Table) by removing non-significant factors, retaining only this three-way interaction as a significant input factor. The p-values from the revised ANOVA table confirmed that the refitted model and the interaction HV*Ton*Toff remained significant for surface roughness.

The interaction between voltage, Ton, and Toff is significant because it influences the spark gap and the energy distribution during the EDM process. Lower voltages (HV) reduce the spark gap and the energy of each discharge, leading to finer surface finishes but potentially lower MRR. When combined with longer Ton, the energy input is increased, which can improve MRR but may also increase surface roughness if not balanced with an appropriate Toff. The study found that optimizing this interaction can minimize surface roughness (Ra) by controlling the energy delivered to the workpiece. For example, a lower voltage combined with longer Ton and a slightly longer Toff can achieve a smoother surface finish by reducing the size of the craters formed during machining. This interaction highlights the need to carefully adjust voltage, pulse duration, and cooling time to achieve the desired surface quality.

Now the main effects plot (Figure) and interaction plot (Figure) were prepared. The main effects plot showed steep slopes of the means, proving the importance of the HV*Ton*Toff interaction on surface roughness. Additionally, the interaction plot exhibited non-parallel lines, confirming that the interaction between these three factors had a significant impact on the output response of Ra.

For optimizing Ra, the target value was set to '0' and the upper bound value was fixed at 0.01 mm, representing the minimum observed value of surface roughness in the experiment. The desirability function (Figure) was applied to check how closely the optimized values aligned with the desired target. A desirability value of d = 0 indicated that the response (Ra) was far from the target of '0', suggesting that the target was not feasible for this response. The response was much lower than the upper bound (0.01 mm), resulting in lower desirability. If the target had been set closer to 0.025 mm, with a larger upper bound (e.g., 0.05 mm), the desirability would have approached one, indicating a more realistic optimization scenario.

Based on this optimization, the following input factors were identified as the optimal values for minimizing surface roughness (Ra):

- Voltage (HV) = 0.70 V
- Pulse on time (Ton) = 6.50 μs
- Pulse off time (Toff) = 6.50 μs

With these optimized values, the minimum surface roughness (Ra) achieved was calculated to be 0.0253 mm. This showed the effectiveness of optimizing these specific parameters for improving surface quality. The interaction of HV, Ton and Toff shows that when voltage and pulse times are balanced, the energy delivered during the machining process becomes more controlled, leading to smaller crater formation and resulting in a smoother surface finish and reduced roughness.

4.1.4 Optimized results for base radius (R). - The base radius (R) for AISI 1045 steel was analyzed using ANOVA in Minitab. The goal was to optimize the output response i.e. base radius. All input factors were considered initially including pulse on time (Ton), pulse off time (Toff) and current (LV. The p-values from the ANOVA Table were assessed, with a threshold of 0.05 for significance. All detailed graphs and table are present in Appendix 6.

Both the ANOVA table (Table), normal probability plot (Figure and Figure) showed that the interaction between LV and Toff (LV*Toff), as well as the three-factor interaction LV, Ton and Toff (LV*Ton*Toff) were significant factors effecting the base radius. The p-values of significant factors are listed below (Table):

- LV*Toff = 0.037
- LV*Ton*Toff = 0.010

The interaction between current and Toff is significant because it reflects the relationship between the intensity of the electrical discharge and the cooling time. Higher currents increase the energy of each spark, leading to higher MRR but also higher electrode wear and surface roughness. When combined with a longer Toff, the cooling time is increased, which can help mitigate the thermal effects of higher currents. The study found that this interaction is particularly important for achieving dimensional accuracy (base radius, R). For example, a higher current combined with a slightly longer Toff can improve material removal efficiency while ensuring sufficient cooling to maintain dimensional accuracy. This interaction emphasizes the need to balance current and cooling time to achieve both productivity and precision.

Now the model (Table) was refitted by eliminating the non-significant factors thus keeping only the significant interactions. The p-values from the refitted ANOVA table confirmed that the revised model and these significant interactions remained statistically valid for optimizing the base radius (R).

After identifying the significant factors, the main effects plot (Figure) and interaction plot (Figure) were generated. The main effects plot displayed a steep slope of means, emphasizing the importance of the interactions between LV, Ton and Toff on the base radius. Similarly, the interaction plot showed non-parallel lines, confirming that the interactions between current, pulse on time and pulse off time had a significant impact on the output response (R).

For optimization, the target value for the base radius was set at 1.5 mm, with an upper bound of 1.55 mm and a lower bound of 1.45 mm, reflecting the desired dimensions of the electrode. The desirability function (Figure) was applied to assess the closeness of the optimized values to the target. A desirability value of d = 0.40233 indicated that the response (R) was about 40% closer to the target, showing a moderate alignment with the desired value of 1.5 mm. Based on the optimization analysis, the following input parameters were determined to be optimal for achieving the desired base radius:

- LV (Current): 30 A
- Ton (Pulse on time): 6.5 µs
- Toff (Pulse off time): 5.5 µs

With these optimized input values, the base radius (R) was calculated to be 1.5298 mm, indicating a close match to the target radius. The interactions between LV, Ton and Toff show that when the current and pulse times are balanced, the material removal process is controlled more precisely thus enabling the electrode to achieve a base radius near the desired dimensions. The non-parallel lines in the interaction plot further reinforce that these factors do not operate independently, but in combination, they significantly influence the output response.

5. Conclusions. - This study aimed to optimize the electrical discharge machining (EDM) process for AISI 1045 steel. A strict focus was on optimization of key output parameters such as machining time (Tm), material removal rate (MRR), electrode wear rate (EWR), surface roughness (Ra) and base radius (R) by. By employing ANOVA analysis in Minitab, significant input factors, including pulse on time (Ton), pulse off time (Toff), current (LV) and voltage (HV), along with their interactions, were systematically analyzed to identify their impact on the five output responses mentioned above. The results of this investigative study provide key insights into how each of these input parameters impact on the five output responses, both individually and in combination, thereby contributing to a more efficient and controlled manufacturing process with the final product being manufactured in less time with reduced material wastages of both workpiece and electrodes and having excellent surface finish. Machining pictures of electrode and workpiece are given in Appendix 9 and Appendix 10.

The optimization of machining time revealed that pulse on time (Ton), its interaction with pulse off time (Ton*Toff) and the three-factor interaction between current, pulse on and pulse off times (LV*Ton*Toff) were the most significant factors affecting Tm. The optimized values of Ton = 6.5 µs, Toff = 5.0 µs and LV = 30A resulted in a minimal machining time of 623.2083 seconds. This showed that while Ton is directly proportional to machining time, specific interactions with Toff and LV can lead to significant reductions in machining time by increasing material removal efficiency.

Similarly, the optimization of the material removal rate (MRR) showed that Ton and the Ton*Toff interaction were significant factors. The optimized parameters, Ton = 6.5 µs and Toff = 5.5 µs, resulted in a maximum MRR of 0.0173 g/min. The relationship between Ton and MRR was found to be directly proportional. This means that with longer pulse durations and higher energy input will lead to more material removal. However, the interaction with Toff required precise timing to ensure that sufficient material was removed without cooling down or solidifying between pulses thus showing the complexity of achieving maximum MRR.

Electrode wear rate (EWR) optimization highlighted that pulse on time (Ton) was the sole significant factor influencing EWR. The optimized value of Ton = 4.0 µs yielded a minimal EWR of 0.0088 g/min, showcasing that shorter pulse durations reduce electrode erosion and prolong electrode life. This result emphasizes the importance of balancing Ton to minimize wear while maintaining machining efficiency.

Surface roughness (Ra) analysis revealed that the interaction between voltage (HV), Ton and Toff (HV*Ton*Toff) was critical in determining surface quality. The optimized values of HV = 0.7V0 V, Ton = 6.5 µs and Toff = 6.5 µs achieved a minimum Ra of 0.0253 mm. This optimization demonstrated that fine control over these interactions reduces crater formation during machining, leading to smoother surface finishes.

Lastly, the base radius (R) optimization showed that the interaction between current (LV) and pulse off time (Toff) (LV*Toff), as well as the three-factor interaction between LV, Ton and Toff (LV*Ton*Toff), were significant in achieving the desired base radius. The optimized values of LV = 30A A, Ton = 6.5 µs and Toff = 5.5 µs resulted in a base radius of 1.5298 mm, closely aligning with the target of 1.5 mm. These findings demonstrate that the precise adjustment of current and pulse timing significantly enhances the dimensional accuracy of the electrode.

In conclusion, this research provides a comprehensive optimization framework for EDM machining of AISI 1045 steel, addressing the critical parameters that influence machining efficiency, quality and precision. By understanding the complex interactions between input parameters, this study offers valuable guidelines for achieving desired machining outcomes while minimizing defects and inefficiencies. The application of these findings in industrial EDM processes can lead to significant improvements in productivity, material usage and overall machining quality.

6. Limitations of the study. - The study has several limitations, including its focus on only four input parameters (Ton, Toff, LV, HV) and AISI 1045 steel, which limits its applicability to other materials and conditions. It did not explore factors like flushing pressure, electrode geometry, or dielectric fluid variations, nor did it consider surface integrity aspects such as recast layer thickness or residual stresses. The experiments were conducted under controlled laboratory conditions, potentially limiting real-world applicability, and the reliance on statistical methods like RSM may not capture complex, non-linear interactions. Additionally, the study did not address economic or environmental impacts, such as cost-effectiveness or the use of kerosene as a dielectric fluid, nor did it compare EDM with other machining methods. These limitations suggest areas for future research to enhance the study's robustness and industrial relevance.

References

[1] *A Review of Recent Application of Machining Techniques, based on the Phenomena of CNC Machining Operations.* I.P. Okokpujie, C.A. Bolu, O.S. Ohunakin, E.T. Akinlabi, D.S. Adelekan. s.l. : Elsevier, 2019, Procedia Manufacturing, Vol. 35, pp. 1054-1060. ISSN 2351-9789.

[2] *Improving the machining performance of polymer hybrid composite by abrasive water jet machining for precise machining.* Kumar, K. Nirmal, and P. Dinesh Babu. s.l. : Springer Nature, 2024, Arabian Journal for Science and Engineering. 2191-4281.

[3] *Ultrasonic machining: a case study.* Gilmore, Randy. 1-2, s.l. : Elsevier, 1991, Journal of Materials Processing Technology, Vol. 28, pp. 139-148. ISSN 0924-0136.

[4] *Mechanical behavior of carbon fiber-reinforced plastic during rotary ultrasonic machining.* Abdelkader Slimane, Mohammed Chaib, Sidahmed Slimane, Sidahmed Dahmane, Anas Abderrahmane Lahouel, Ahmed Guelailia, Kaddour Bahram, Said Kebdani & Benattou Bouchouicha. 11, s.l. : Springer Nature, 2024, The International Journal of Advanced Manufacturing Technology, Vol. 130, pp. 5345-5357. 1433-3015.

[5] *A comprehensive review of studying the influence of laser cutting parameters on surface and kerf quality of metals.* Muhammad Alsaadawy, Montasser Dewidar, Ahmed Said, Ibrahem Maher & Taher A. Shehabeldeen. 3, s.l. : Springer Nature, 2024, The International Journal of Advanced Manufacturing Technology, Vol. 130, pp. 1039-1074.

[6] *Innovation Study for Laser Cutting of Complex Geometries with Paper Materials.* A. Happonen, A. Stepanov, H. Piili, A. Salminen. s.l. : Elsevier, 2015, Physics Procedia, Vol. 78, pp. 128-137. ISSN 1875-3892.

[7] *Electric Discharge Machining of Ti6Al4V ELI in Biomedical Industry: Parametric Analysis of Surface Functionalization and Tribological Characterization.* Farooq, Muhammad Umar, Saqib Anwar, Haider Ali Bhatti, M. Saravana Kumar, Muhammad Asad Ali, and Muhammad Imam Ammarullah. 12, s.l. : MDPI, 2023, Materials, Vol. 16. 1996-1944.

[8] *Optimization design for die-sinking EDM process parameters employing effective intelligent method.* Van Tron Tran, Minh Huy Le,Minh Thai Vo,Quoc Trung Le,Van Huong Hoang,Ngoc-Thien Tran,Van-Thuc Nguyen,Thi-Anh-Tuyet Nguyen,Hoai Nam Nguyen,Van Thanh Tien NguyenORCID Icon &Thanh Tan Nguyen. 2, s.l. : Taylor & Francis, 2023, Cogent engineering, Vol. 10.

[9] *Experimental Study on Electrochemical Machining with Electrolyte Confined by Absorption Material.* Wataru Natsu, Junfeng He, Yu Iwanaga. s.l. : Elsevier, 2020, Procedia CIRP, Vol. 87, pp. 263-267.

[10] *A review on recent achievements and challenges in electrochemical machining of tungsten carbide.* Mohammed Asmael, Amin Memarzadeh. 1, s.l. : Queens University Belfast, 2023, Archives of Advanced Engineering Science, Vol. 2, pp. 1-23.

[11] *To Study the Effect of Process Parameters for Minimum Surface Roughness of Cylindrical Grinded AISI 1045 Steel.* Singh, T., Goyal, K., Kumar, P. 3, s.l. : Horizon Research Publishing Corporation, 2014, Manufacturing Science and Technology, Vol. 2, pp. 56-61.

[12] *Surface texturing of the carbon steel AISI 1045 using femtosecond laser in single pulse and scanning regime.* Stašić J, Gaković B, Perrie W, Watkins K, Petrović S, Trtica M. 1, s.l. : Elsevier, 2011, Applied Surface Science, Vol. 258, pp. 290-296. ISSN 0169-4332.

[13] *A Review of Electrode Manufacturing Methods for Electrical Discharge Machining: Current Status and Future Perspectives for Surface Alloying.* Garba, E., et al. 9, s.l. : MDPI, 2023, Machines, Vol. 11. 906.

[14] *Experimental Investigations of Surface Modification of AISI 1045 Die Steel by Electro Discharge Machining Process.* Harjot Singh, S.S. Banwait. 4, s.l. : Science and Education Publishing Co., 2016, American Journal of Mechanical Engineering, Vol. 4, pp. 131-141.

[15] *Prediction and optimization of performance measures in electrical discharge machining using rapid prototyping tool electrodes.* Mahapatra, Anshuman Kumar Sahu & Siba Sankar. s.l. : Springer Nature, 2021, Journal of Intelligent Manufacturing, Vol. 32, pp. 2125-2145.

[16] *Reviewing performance measures of the die-sinking electrical discharge machining process: challenges and future scopes.* Shastri, R.K., et al. 384, s.l. : MDPI, 2022, Nanomaterials, Vol. 12.

[17] *Process optimization for rapid manufacturing of complex geometry electrical discharge machining electrode.* Singh J, Pandey PM. 1, s.l. : Sage Journals, 2020, Proceedings of the Institution of Mechanical Engineers, Part C: Journal of Mechanical Engineering Science, Vol. 231, pp. 66-81.

[18] *Influence of ZnO nanoparticle addition and spark peak current on EDM process of AISI 1045, AISI 4140, and AISI D3: MRR, surface roughness, and surface topography.* K., Masoud Pour & S. Ehsan Layegh. s.l. : Springer Nature, 2022, The International Journal of Advanced Manufacturing Technology , Vol. 122, pp. 3703-3724.

[19] *Electrical Discharge Machining (EDM): A Review.* Banu, A., & Ali, M. Y. 1, s.l. : Deer Hill Publications, 2016, International Journal of Engineering Materials and Manufacture, Vol. 1, pp. 3-10. E-ISSN: 0128-1852.

[20] *Wire EDM process optimization for machining AISI 1045 steel by use of Taguchi method, artificial neural network and analysis of variances.* Ahmed A. A. Alduroobi, Alaa M. Ubaid, Maan Aabid Tawfiq & Rasha R. Elias. 6, s.l. : Springer Nature, 2020, International Journal of System Assurance Engineering and Management , Vol. 11, pp. 1314-1338. 0976-4348.

[21] *Study on AISI1045 material for various applications: an over view.* Vishnuja, U., Bhaskar, GB. 2, s.l. : Research India Publivcations, 2018, International Journal of Engineering and Manufacturing, Vol. 8, pp. 125-144. ISSN 2249-3115.

[22] *Investigation on the influence of machining parameters when machining tool steel using EDM.* C.H. Che Haron, B.Md. Deros, A. Ginting, M. Fauziah. 1, s.l. : Elsevier, 2001, Journal of Materials Processing Technology, Vol. 116, pp. 84-87.

[23] *Optimization of Machining Parameters for Surface Roughness in EDM of AISI 1045 Based on Taguchi Technique.* Agarwal, Subodh Kumar and Sanjay. Vancouver, British Columbia, Canada : ASME, 2012. ASME International Mechanical Engineering Congress & Exposition. Vol. 3. ISBN: 978-0-7918-4427-4.

[24] *Optimization of wire electric discharge machining (WEDM) process parameters for AISI 1045 medium carbon steel using Taguchi design of experiments.* Zaman, Uzair Khaleeq uz, Usman Ahmed Khan, Shahid Aziz, Aamer Ahmed Baqai, Sajid Ullah Butt, Danish Hussain, Ali Siadat, and Dong Won Jung. 21, s.l. : MDPI, 2022, Materials, Vol. 15. 7846.

[25] *Variation of surface roughness on electrical discharge machining die sinking caused of different electrode material, current, and on Time.* Darsin, M., Y. Hermawan, and A. Rachmat. Bali, Indonesia : Asian Federation of Biotechnology, 2011. 12th International Conference on Quality in Research. pp. 956-961. ISSN 114-1284.

[26] *Application of Response Surface Methodology For Determining MRR and TWR Model In Die Sinking EDM of AISI 1045 Steel.* M. B. Patel, P. K. Patel, J. B. Patel, B. B. Patel. 6, 2012, International Journal of Engineering Research and Applications, Vol. 2, pp. 1227-1231. ISSN: 2248-9622.

[27] *Analysis of material removal rate and electrode wear in sinking EDM roughing strategies using different graphite grades.* F Klocke, M Schwade, A Klink, D Veselovac. [ed.] J.-P. Kruth B. Lauwers. Leuven, Belgium : Elsevier, 2013. Proceedings of the Seventeenth CIRP Conference on Electro Physical and Chemical Machining (ISEM). Vol. 6, pp. 163-167. ISSN 2212-8271.

[28] *Modeling and analysis of MRR, EWR and surface roughness in EDM milling through response surface methodology.* Khan, A.K.M. Asif Iqbal and Ahsan Ali. 4, s.l. : Science Publications, 2010, American Journal of Engineering and Applied Sciences, Vol. 3, pp. 611-619. ISSN 1941-7020 .

Appendix 1

RUN	LV	HV	PULSE ON TIME	PULSE OFF TIME
1	0.3	30	4	5.5
2	0.7	30	4	5.5
3	0.3	50	4	5.5
4	0.7	50	4	5.5
5	0.3	30	6.5	5.5
6	0.7	30	6.5	5.5
7	0.3	50	6.5	5.5
8	0.7	50	6.5	5.5
9	0.3	30	4	6.5
10	0.7	30	4	6.5
11	0.3	50	4	6.5
12	0.7	50	4	6.5
13	0.3	30	6.5	6.5
14	0.7	30	6.5	6.5
15	0.3	50	6.5	6.5
16	0.7	50	6.5	6.5

Table III. Basic experimental runs for AISI-1045

Appendix 2

Factorial Fit: Tm versus HV, LV, Ton, Toff

Estimated Effects and Coefficients for Tm (coded units)

Term	Effect	Coef	SE Coef	T	P
Constant		845.6	24.05	35.16	0.000
HV	23.5	11.7	24.05	0.49	0.629
LV	-60.8	-30.4	24.05	-1.26	0.215
Ton	-261.0	-130.5	24.05	-5.43	0.000
Toff	21.0	10.5	24.05	0.44	0.666
HV*LV	-7.5	-3.8	24.05	-0.16	0.876
HV*Ton	-29.2	-14.6	24.05	-0.61	0.548
HV*Toff	-1.0	-0.5	24.05	-0.02	0.984
LV*Ton	-76.0	-38.0	24.05	-1.58	0.124
LV*Toff	85.6	42.8	24.05	1.78	0.085
Ton*Toff	113.3	56.6	24.05	2.36	0.025
HV*LV*Ton	-19.5	-9.8	24.05	-0.41	0.687
HV*LV*Toff	21.0	10.5	24.05	0.44	0.665
HV*Ton*Toff	-40.5	-20.2	24.05	-0.84	0.407
LV*Ton*Toff	-110.4	-55.2	24.05	-2.29	0.028
HV*LV*Ton*Toff	-53.8	-26.9	24.05	-1.12	0.272

S = 166.624 R-Sq = 61.28% R-Sq(adj) = 43.13%

Analysis of Variance for Tm (coded units)

Source	DF	SeqSS	Adj SS	Adj MS	F	P
Main Effects	4	873413	873413	218353	7.86	0.000
2-Way Interactions	6	322167	322167	53694	1.93	0.105
3-Way Interactions	4	175730	175730	43932	1.58	0.203
4-Way Interactions	1	34723	34723	34723	1.25	0.272
Residual Error	32	888437	888437	27764		
Pure Error	32	888437	888437	27764		
Total	47	2294469				

Unusual Observations for Tm

Obs	StdOrder	Tm	Fit	SE Fit	Residual	St Resid
9	9	495.00	821.67	96.20	-326.67	-2.40R
36	36	1231.00	907.00	96.20	324.00	2.38R

R denotes an observation with a large standardized residual.

Table IV. ANOVA Table of Tm for AISI-1045 considering all factors.

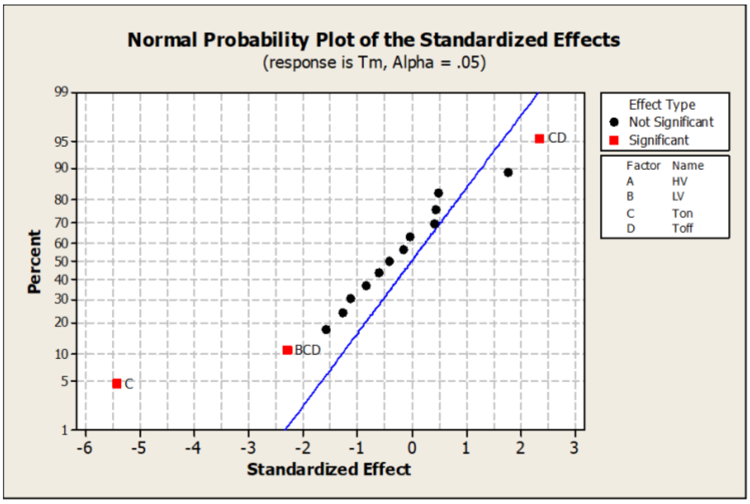

Figure VII. Normal Probability Plot of the standardized effects of Tm for AISI-1045 considering all factors.

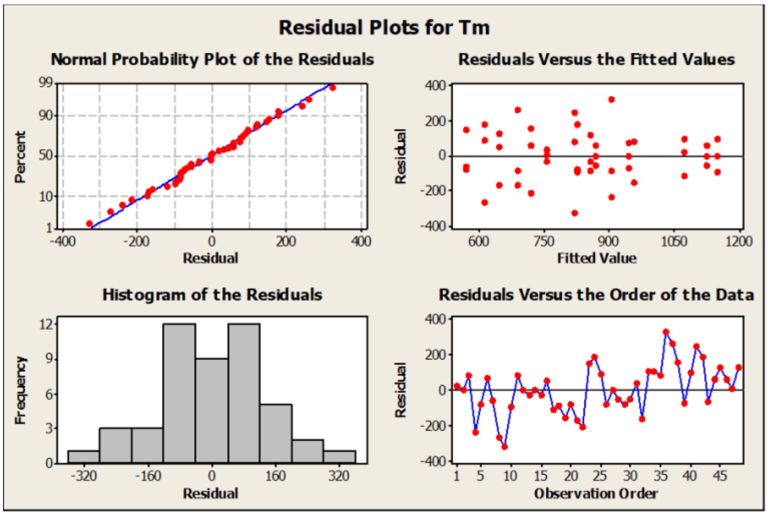

Figure VIII. Residual Plot of Tm for AISI-1045 considering all factors.

Factorial Fit: Tm versus LV, Ton, Toff

Estimated Effects and Coefficients for Tm (coded units)

Term	Effect	Coef	SE Coef	T	P
Constant		845.6	23.65	35.76	0.000
LV	-60.8	-30.4	23.65	-1.29	0.206
Ton	-261.0	-130.5	23.65	-5.52	0.000
Toff	21.0	10.5	23.65	0.44	0.660
Ton*Toff	113.3	56.6	23.65	2.40	0.021
LV*Ton*Toff	-110.4	-55.2	23.65	-2.33	0.024

S = 163.841   R-Sq = 50.86%   R-Sq(adj) = 45.01%

Analysis of Variance for Tm (coded units)

Source	DF	Seq SS	AdjSS	MS	F	P
Main Effects	3	866810	866810	288937	10.76	0.000
2-Way Interactions	1	154020	154020	154020	5.74	0.021
3-Way Interactions	1	146192	146192	146192	5.45	0.024
Residual Error	42	1127448	1127448	26844		
Lack of Fit	2	157216	157216	78608	3.24	0.050
Pure Error	40	970233	970233	24256		
Total	47	2294469				

Unusual Observations for Tm

Obs	StdOrder	Tm	Fit	SE Fit	Residual	St Resid
4	4	668.00	1022.80	59.92	-354.80	-2.33R
9	9	495.00	942.40	55.34	-447.40	-2.90R

R denotes an observation with a large standardized residual.

Estimated Coefficients for Tm using data in uncoded units

Term	Coef
Constant	3833.95
LV	7.22155
Ton	-648.183
Toff	-454.867
Ton*Toff	103.663
LV*Ton*Toff	-0.325750

Table V. ANOVA Table of Tm for AISI-1045 considering significant factors.

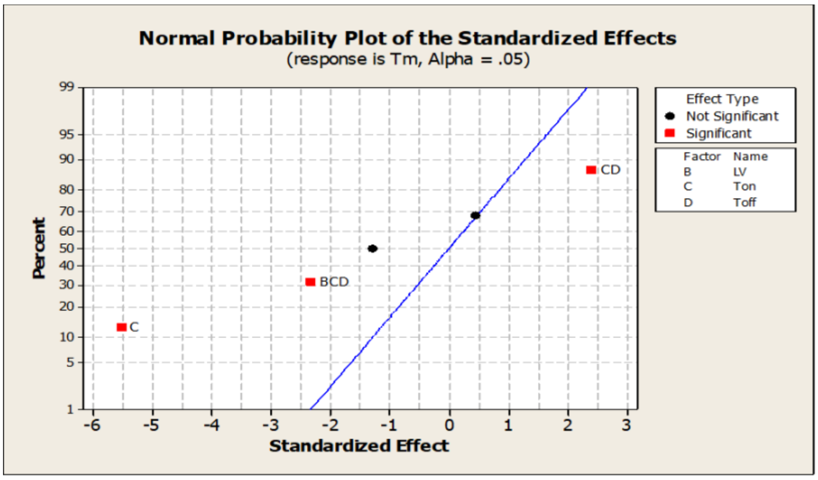

Figure IX. Normal Probability Plot of the standardized effects of Tm for AISI-1045 considering significant factors.

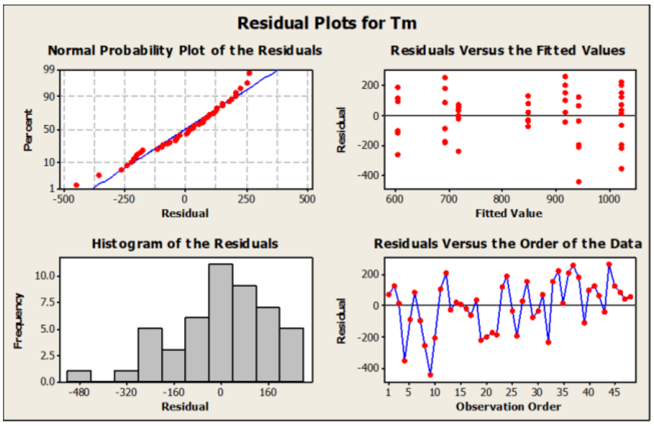

Figure X. Residual Plot of Tm for AISI-1045 considering all factors.

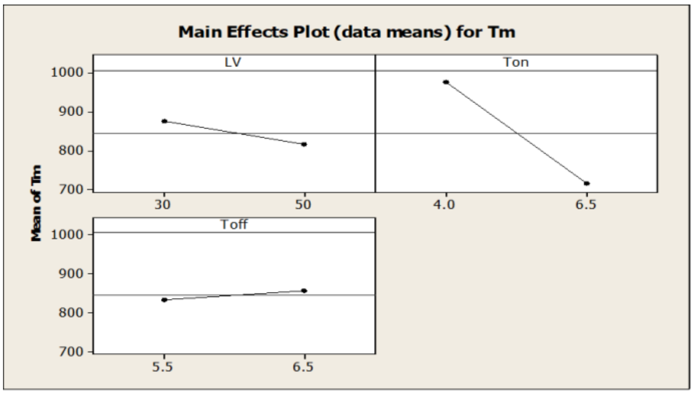

Figure XI. Main Effects Plot of Tm for AISI-1045 considering significant factors.

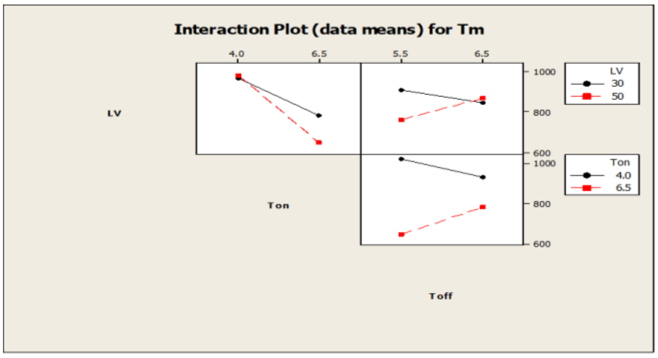

Figure XII. Residual Plot of Tm for AISI-1045 considering Ton & LV.

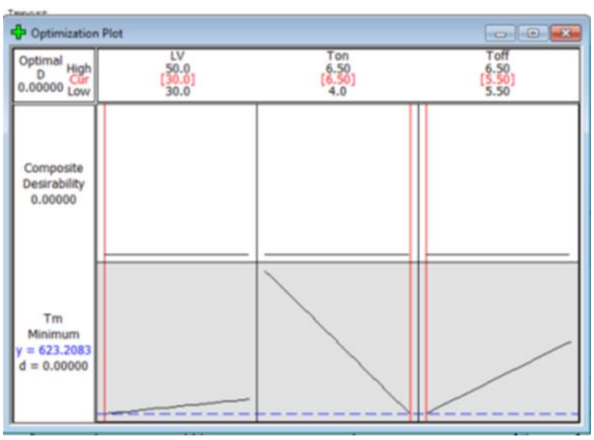

Figure XIII. Optimization Plot of Tm for AISI-1045 for significant factors

Appendix 3

Factorial Fit: MRR versus HV, LV, Ton, Toff

Estimated Effects and Coefficients for MRR (coded units)

Term	Effect	Coef	SE Coef	T	P
Constant		0.012883	0.000575	22.41	0.000
HV	0.000160	0.000080	0.000575	0.14	0.890
LV	0.001598	0.000799	0.000575	1.39	0.174
Ton	0.004607	0.002304	0.000575	4.01	0.000
Toff	-0.001590	-0.000795	0.000575	-1.38	0.176
HV*LV	0.000896	0.000448	0.000575	0.78	0.441
HV*Ton	0.000844	0.000422	0.000575	0.73	0.468
HV*Toff	-0.000010	-0.000005	0.000575	-0.01	0.993
LV*Ton	0.001988	0.000994	0.000575	1.73	0.093
LV*Toff	-0.001694	-0.000847	0.000575	-1.47	0.151
Ton*Toff	-0.002541	-0.001271	0.000575	-2.21	0.034
HV*LV*Ton	0.000405	0.000202	0.000575	0.35	0.727
HV*LV*Toff	0.000083	0.000041	0.000575	0.07	0.943
HV*Ton*Toff	0.000814	0.000407	0.000575	0.71	0.484
LV*Ton*Toff	0.000966	0.000483	0.000575	0.84	0.407
HV*LV*Ton*Toff	0.000795	0.000397	0.000575	0.69	0.495

S = 0.00398335   R-Sq = 50.71%   R-Sq(adj) = 27.60%

Analysis of Variance for MRR (coded units)

Source	DF	Seq SS	Adj SS	Adj MS	F	P
Main Effects	4	0.00031597	0.00031597	0.00007899	4.98	0.003
2-Way Interactions	6	0.00017753	0.00017753	0.00002959	1.86	0.118
3-Way Interactions	4	0.00002120	0.00002120	0.00000530	0.33	0.853
4-Way Interactions	1	0.00000758	0.00000758	0.00000758	0.48	0.495
Residual Error	32	0.00050775	0.00050775	0.00001587		
Pure Error	32	0.00050775	0.00050775	0.00001587		
Total	47	0.00103002				

Unusual Observations for MRR

Obs	StdOrder	MRR	Fit	SE Fit	Residual	StResid
8	8	0.031840	0.019720	0.002300	0.012120	3.73R
24	24	0.012790	0.019720	0.002300	-0.006930	-2.13R

R denotes an observation with a large standardized residual.

Table VI. ANOVA Table of MRR for AISI-1045 considering all factors.

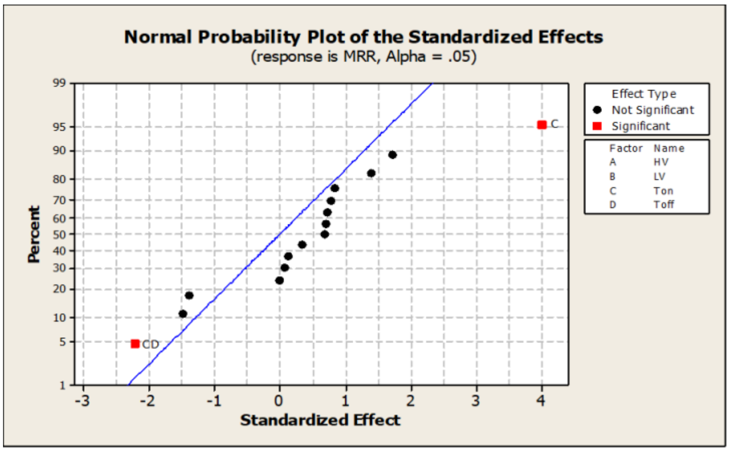

Figure XIV. Normal Probability Plot of the standardized effects of MRR for AISI-1045 considering all factors.

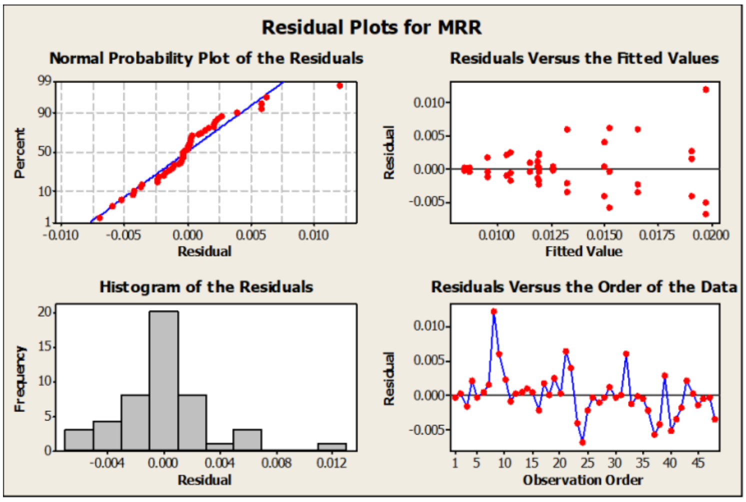

Figure XV. Residual Plot of MRR for AISI-1045 considering all factors.

Factorial Fit: MRR versus Ton, Toff

Estimated Effects and Coefficients for MRR (coded units)

Term	Effect	Coef	SE Coef	T	P
Constant		0.012883	0.000562	22.92	0.000
Ton	0.004607	0.002304	0.000562	4.10	0.000
Toff	-0.001590	-0.000795	0.000562	-1.41	0.164
Ton*Toff	-0.002541	-0.001271	0.000562	-2.26	0.029

S = 0.00389492   R-Sq = 35.20%   R-Sq(adj) = 30.78%

Analysis of Variance for MRR (coded units)

Source	DF	Seq SS	Adj SS	Adj MS	F	P
Main Effects	2	0.00028502	0.00028502	0.00014251	9.39	0.000
2-Way Interactions	1	0.00007750	0.00007750	0.00007750	5.11	0.029
Residual Error	44	0.00066750	0.00066750	0.00001517		

Pure Error 44 0.00066750 0.00066750 0.00001517
Total 47 0.00103002

Unusual Observations for MRR

ObsStdOrder		MRR	Fit	SE Fit	Residual	StResid
8	8	0.031840	0.017252	0.001124	0.014588	3.91R
9	9	0.019150	0.011055	0.001124	0.008095	2.17R
32	32	0.022470	0.013121	0.001124	0.009349	2.51R
37	37	0.009300	0.017252	0.001124	-0.007952	-2.13R

R denotes an observation with a large standardized residual.

Estimated Coefficients for MRR using data in uncoded units

Term	Coef
Constant	-0.0512942

Table VII. ANOVA Table of MRR for AISI-1045 considering significant factors.

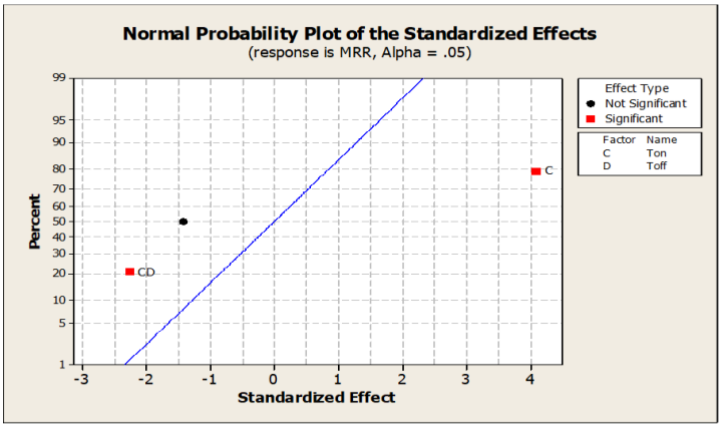

Figure XVI. Normal Probability Plot of the standardized effects of MRR for AISI-1045 considering significant factors

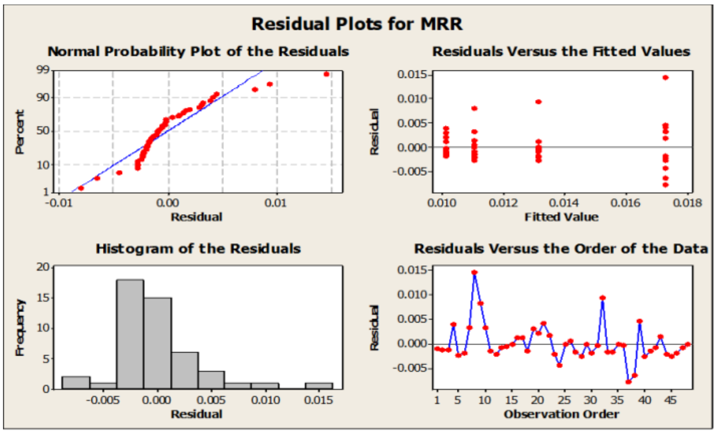

Figure XVII. Residual Plot of MRR for AISI-1045 considering all factors.

https://doi.org/10.36561/ING.28.15
ISSN 2301-1092 • ISSN (en línea) 2301-1106 – Universidad de Montevideo, Uruguay

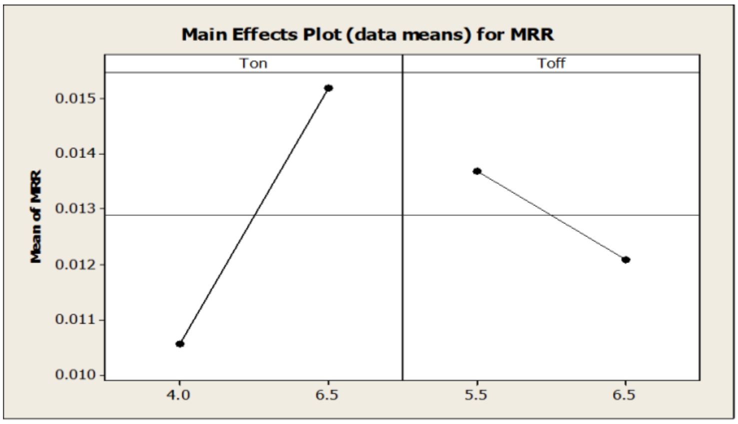

Figure XVIII. Main Effects Plot of MRR for AISI-1045 considering significant factors.

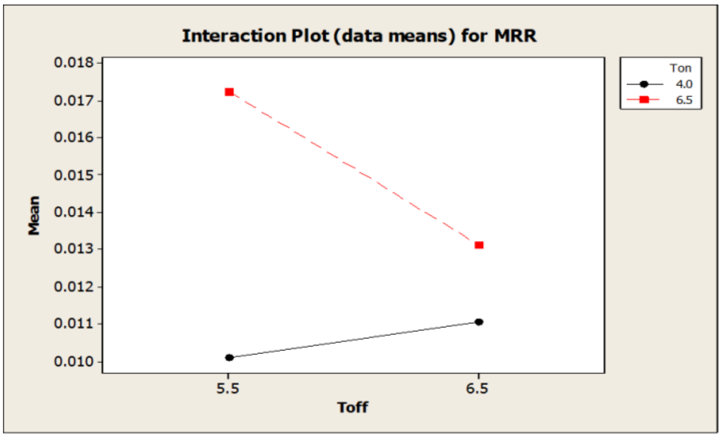

Figure XIX. Residual Plot of MRR for AISI-1045 considering Ton & LV.

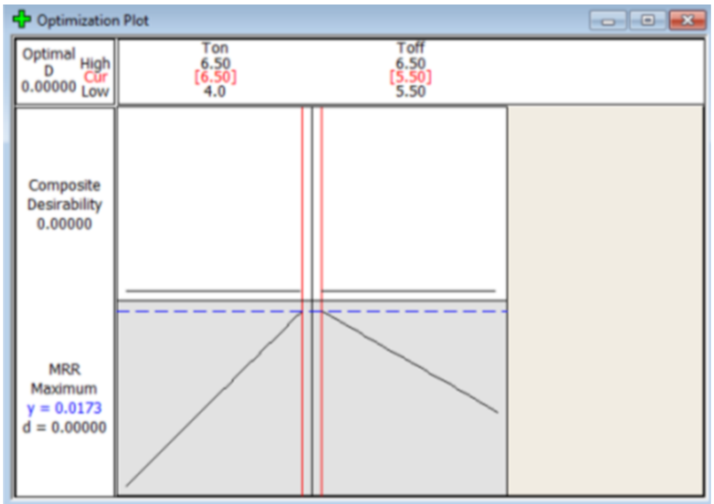

Figure XX. Optimization Plot of MRR for AISI-1045 for significant factors.

Appendix 4

Factorial Fit: EWR versus HV, LV, Ton, Toff

Estimated Effects and Coefficients for EW (coded units)

Term	Effect	Coef	SE Coef	T	P
Constant		0.010172	0.000382	26.66	0.000
HV	-0.000559	-0.000279	0.000382	-0.73	0.469
LV	0.001468	0.000734	0.000382	1.92	0.063
Ton	0.002742	0.001371	0.000382	3.59	0.001
Toff	-0.000344	-0.000172	0.000382	-0.45	0.655
HV*LV	0.000028	0.000014	0.000382	0.04	0.971
HV*Ton	0.000919	0.000459	0.000382	1.20	0.238
HV*Toff	0.000263	0.000131	0.000382	0.34	0.733
LV*Ton	0.001214	0.000607	0.000382	1.59	0.122
LV*Toff	-0.001214	-0.000607	0.000382	-1.59	0.122
Ton*Toff	-0.001386	-0.000693	0.000382	-1.82	0.079
HV*LV*Ton	0.000284	0.000142	0.000382	0.37	0.713
HV*LV*Toff	0.000583	0.000291	0.000382	0.76	0.451
HV*Ton*Toff	0.000227	0.000114	0.000382	0.30	0.768
LV*Ton*Toff	0.001205	0.000603	0.000382	1.58	0.124
HV*LV*Ton*Toff	-0.000048	-0.000024	0.000382	-0.06	0.950

S = 0.00264388 PRESS = 0.000503286
R-Sq = 48.87% R-Sq(pred) = 0.00% R-Sq(adj) = 24.90%

Analysis of Variance for EW (coded units)

Source	DF	Seq SS	Adj SS	Adj MS	F	P
Main Effects	4	0.00012125	0.00012125	0.00003031	4.34	0.006
2-Way Interactions	6	0.00006938	0.00006938	0.00001156	1.65	0.165
3-Way Interactions	4	0.00002310	0.00002310	0.00000577	0.83	0.518
4-Way Interactions	1	0.00000003	0.00000003	0.00000003	0.00	0.950
Residual Error	32	0.00022368	0.00022368	0.00000699		
Pure Error	32	0.00022368	0.00022368	0.00000699		
Total	47	0.00043744				

Unusual Observations for EW

Obs	StdOrder	EW	Fit	SE Fit	Residual	St Resid
8	8	0.019770	0.013577	0.001526	0.006193	2.87R
9	9	0.016610	0.011313	0.001526	0.005297	2.45R

R denotes an observation with a large standardized residual.

Table VIII. ANOVA Table of EWR for AISI-1045 considering all factors.

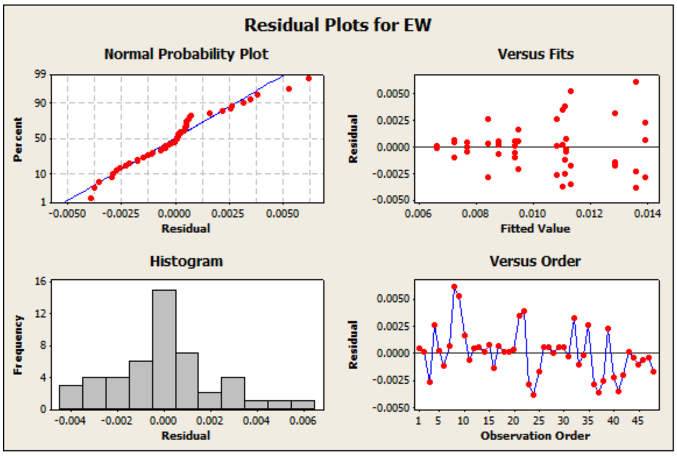

Figure XXI. Residual Plot of EW for AISI-1045 considering all factors.

Factorial Fit: EWR versus Ton

Estimated Effects and Coefficients for EW (coded units)

Term	Effect	Coef	SE Coef	T	P
Constant		0.010172	0.000397	25.65	0.000
Ton	0.002742	0.001371	0.000397	3.46	0.001

S = 0.00274739   PRESS = 0.000378065

R-Sq = 20.63%   R-Sq(pred) = 13.57%   R-Sq(adj) = 18.90%

Analysis of Variance for EW (coded units)

Source	DF	Seq SS	Adj SS	Adj MS	F	P
Main Effects	1	0.00009023	0.00009023	0.00009023	11.95	0.001
Residual Error	46	0.00034722	0.00034722	0.00000755		
Pure Error	46	0.00034722	0.00034722	0.00000755		
Total	47	0.00043744				

Unusual Observations for EW

Obs	StdOrder	EW	Fit	SE Fit	Residual	St Resid
8	8	0.019770	0.011543	0.000561	0.008227	3.06R
9	9	0.016610	0.008801	0.000561	0.007809	2.90R

R denotes an observation with a large standardized residual.

Estimated Coefficients for EW using data in uncoded units

Term	Coef
Constant	0.00441392
Ton	0.00109683

Table IX. Table of EWR for AISI-1045 considering significant factors.

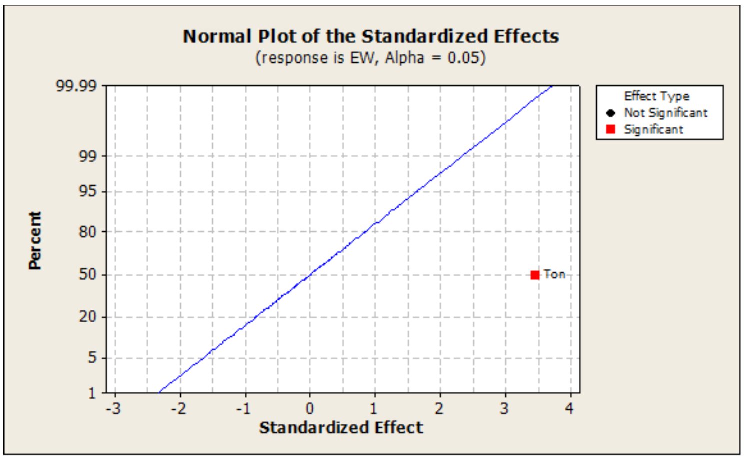

Figure XXII. Normal Probability Plot of the standardized effects ofAISI-1045 for AISI 1045 considering significant factors.

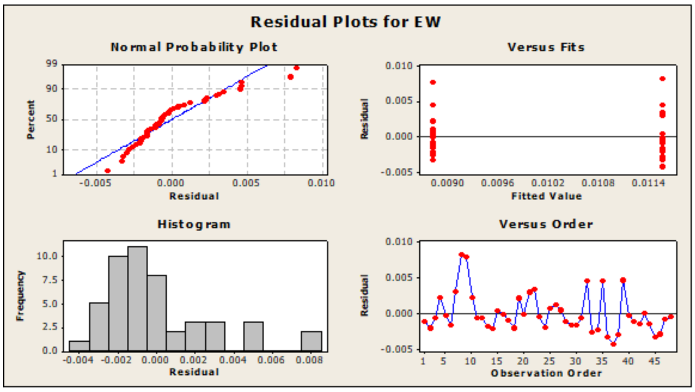

Figure XXIII. Residual Plot of EWR for AISI-1045 considering all factors.

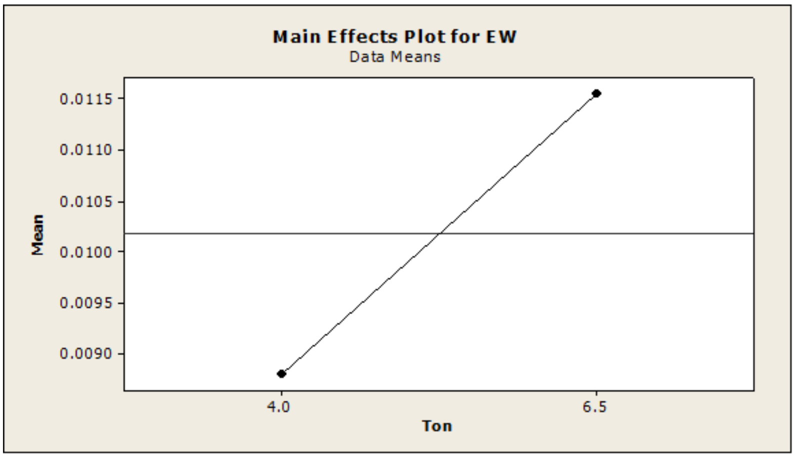

Figure XXIV. Main Effects Plot of EWR for AISI-1045 considering significant factors.

https://doi.org/10.36561/ING.28.15
ISSN 2301-1092 • ISSN (en línea) 2301-1106 – Universidad de Montevideo, Uruguay

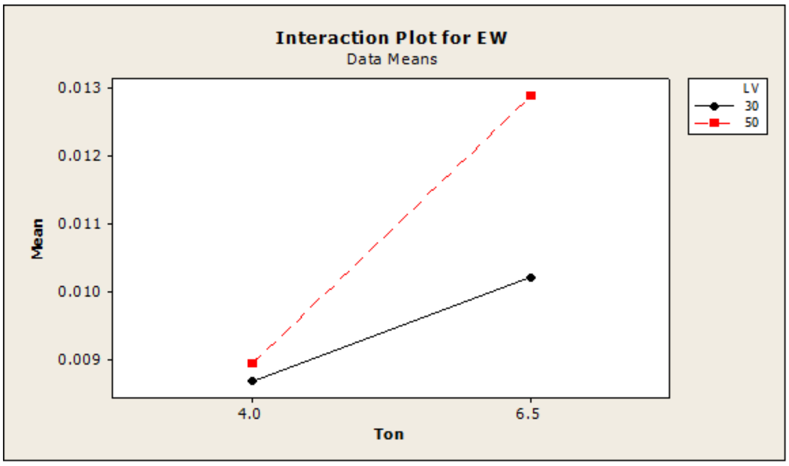

Figure XXV. Residual Plot of EWR for AISI-1045 considering Ton & LV.

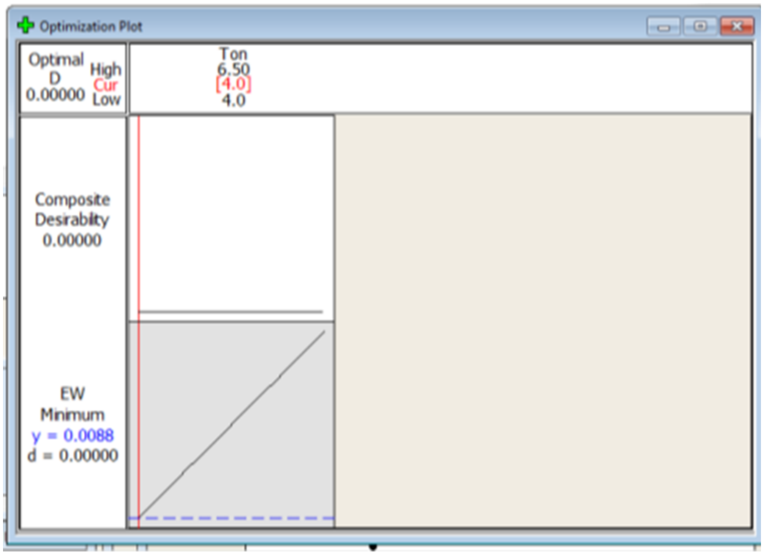

Figure XXVI. Optimization Plot of EWR for AISI-1045 for significant factors.

Appendix 5

Factorial Fit: Ra versus HV, LV, Ton, Toff

Estimated Effects and Coefficients for Ra (coded units)

Term	Effect	Coef	SE Coef	T	P
Constant		0.03696	0.004893	7.55	0.000
HV	0.00167	0.00083	0.004893	0.17	0.866
LV	-0.00367	-0.00183	0.004893	-0.37	0.710
Ton	-0.00175	-0.00088	0.004893	-0.18	0.859
Toff	-0.00217	-0.00108	0.004893	-0.22	0.826
HV*LV	0.00675	0.00337	0.004893	0.69	0.495
HV*Ton	0.01433	0.00717	0.004893	1.46	0.153
HV*Toff	0.01158	0.00579	0.004893	1.18	0.245
LV*Ton	0.01183	0.00592	0.004893	1.21	0.235
LV*Toff	0.00358	0.00179	0.004893	0.37	0.717
Ton*Toff	0.00483	0.00242	0.004893	0.49	0.625
HV*LV*Ton	-0.00908	-0.00454	0.004893	-0.93	0.360
HV*LV*Toff	-0.01467	-0.00733	0.004893	-1.50	0.144
HV*Ton*Toff	-0.02108	-0.01054	0.004893	-2.15	0.039
LV*Ton*Toff	-0.00858	-0.00429	0.004893	-0.88	0.387
HV*LV*Ton*Toff	0.01050	0.00525	0.004893	1.07	0.291

S = 0.0339027   PRESS = 0.0827565
R-Sq = 33.03%   R-Sq(pred) = 0.00%   R-Sq(adj) = 1.63%

Analysis of Variance for Ra (coded units)

Source	DF	Seq SS	Adj SS	Adj MS	F	P
Main Effects	4	0.0002878	0.0002878	0.00007194	0.06	0.992
2-Way Interactions	6	0.0067369	0.0067369	0.00112282	0.98	0.457
3-Way Interactions	4	0.0097896	0.0097896	0.00244740	2.13	0.100
4-Way Interactions	1	0.0013230	0.0013230	0.00132300	1.15	0.291
Residual Error	32	0.0367807	0.0367807	0.00114940		
Pure Error	32	0.0367807	0.0367807	0.00114940		
Total	47	0.0549179				

Unusual Observations for Ra

Obs	StdOrder	Ra	Fit	SE Fit	Residual	StResid
1	1	0.042000	0.098333	0.019574	-0.056333	-2.04R
17	17	0.230000	0.098333	0.019574	0.131667	4.76R
24	24	0.111000	0.055000	0.019574	0.056000	2.02R
33	33	0.023000	0.098333	0.019574	-0.075333	-2.72R

R denotes an observation with a large standardized residual.

Table X. ANOVA Table of Ra for AISI-1045 considering all factors.

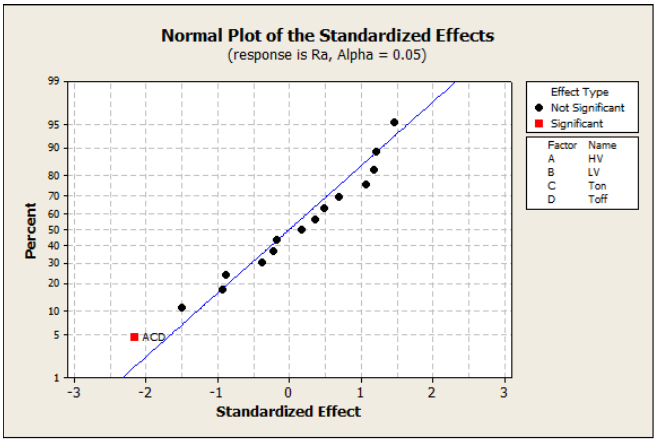

Figure XXVII. Normal Probability Plot of the standardized effects of Ra for AISI-1045 considering all factors.

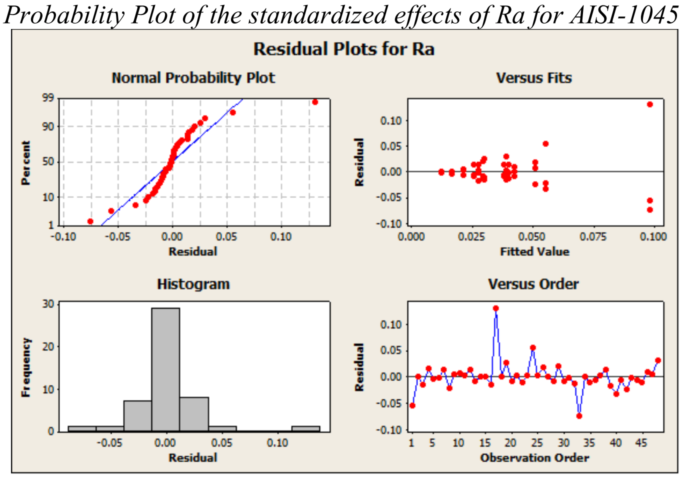

Figure XXVIII. Residual Plot of Ra for AISI-1045 considering all factors.

Factorial Fit: Ra versus HV, Ton, Toff

Estimated Effects and Coefficients for Ra (coded units)

Term	Effect	Coef	SE Coef	T	P
Constant		0.03696	0.004895	7.55	0.000
HV	0.00167	0.00083	0.004895	0.17	0.866
Ton	-0.00175	-0.00088	0.004895	-0.18	0.859
Toff	-0.00217	-0.00108	0.004895	-0.22	0.826
HV*Ton*Toff	-0.02108	-0.01054	0.004895	-2.15	0.037

S = 0.0339142 PRESS = 0.0616278

R-Sq = 9.94% R-Sq(pred) = 0.00% R-Sq(adj) = 1.57%

Analysis of Variance for Ra (coded units)

Source	DF	Seq SS	Adj SS	Adj MS	F	P
Main Effects	3	0.0001264	0.0001264	0.00004214	0.04	0.990
3-Way Interactions	1	0.0053341	0.0053341	0.00533408	4.64	0.037
Residual Error	43	0.0494574	0.0494574	0.00115017		
Lack of Fit	3	0.0043558	0.0043558	0.00145192	1.29	0.292

```
 Pure Error      40  0.0451017  0.0451017  0.00112754
Total            47  0.0549179

Unusual Observations for Ra
ObsStdOrder       Ra       Fit    SE Fit      Residual  St Resid
 17        17  0.230000  0.048625  0.010946  0.181375      5.65R
R denotes an observation with a large standardized residual.

* NOTE * Estimated regression coefficients in uncoded units are not available
because the model is non-hierarchical.
```

Table XI. ANOVA Table of Ra for AISI-1045 considering significant factors.

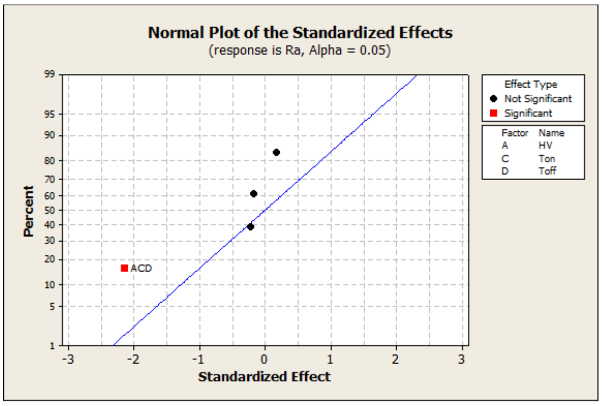

Figure XXIX. Normal Probability Plot of the standardized effects of Ra for AISI-1045 considering significant factors.

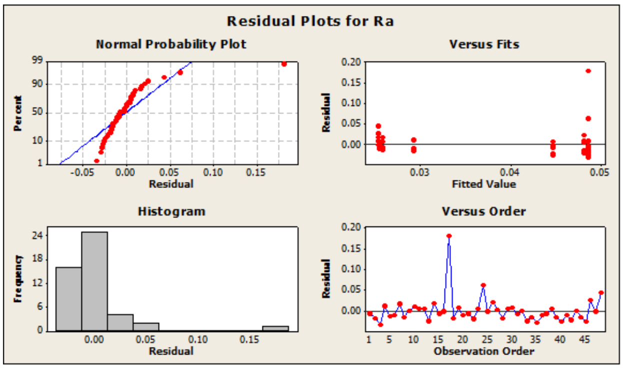

Figure XXX. Residual Plot of Ra for AISI-1045 considering significant factors.

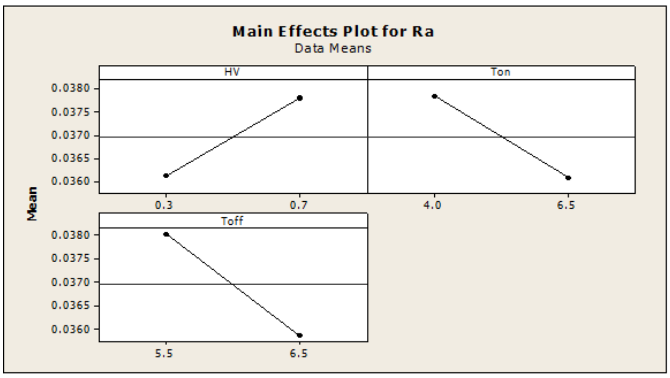

Figure XXXI. Main Effects Plot of Ra for AISI-1045 considering significant factors.

Memoria Investigaciones en Ingeniería, núm. 28 (2025). pp. 222-268
https://doi.org/10.36561/ING.28.15
ISSN 2301-1092 • ISSN (en línea) 2301-1106 – Universidad de Montevideo, Uruguay

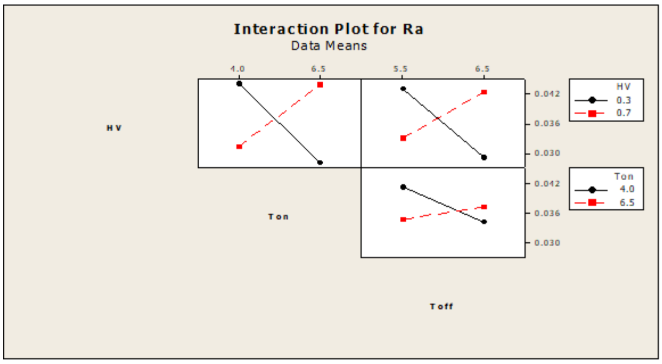

Figure XXXII. Residual Plot of Ra for AISI-1045 considering HV, Ton &Toff.

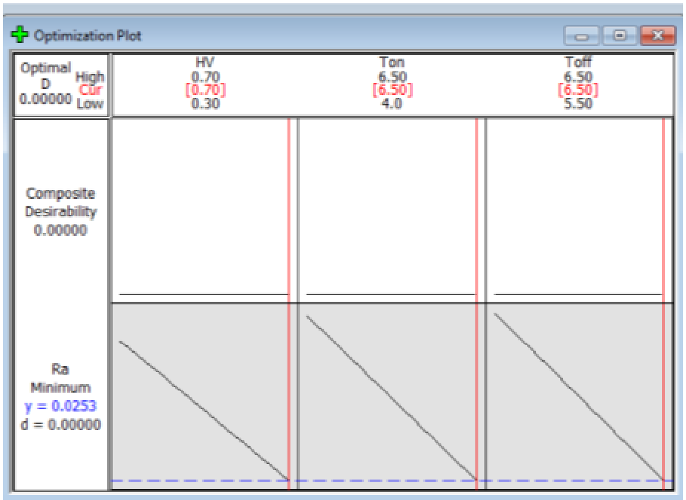

Figure XXXIII. Optimization Plot of Ra for AISI-1045 for significant factors.

Appendix 6

Factorial Fit: R versus HV, LV, Ton, Toff

Estimated Effects and Coefficients for R (coded units)

Term	Effect	Coef	SE Coef	T	P
Constant		1.55752	0.004904	317.62	0.000
HV	-0.00396	-0.00198	0.004904	-0.40	0.689
LV	0.00754	0.00377	0.004904	0.77	0.448
Ton	0.00304	0.00152	0.004904	0.31	0.758
Toff	0.00246	0.00123	0.004904	0.25	0.804
HV*LV	-0.00196	-0.00098	0.004904	-0.20	0.843
HV*Ton	0.00421	0.00210	0.004904	0.43	0.671
HV*Toff	-0.00521	-0.00260	0.004904	-0.53	0.599
LV*Ton	0.00304	0.00152	0.004904	0.31	0.758
LV*Toff	-0.02138	-0.01069	0.004904	-2.18	0.037
Ton*Toff	0.00096	0.00048	0.004904	0.10	0.923
HV*LV*Ton	0.01504	0.00752	0.004904	1.53	0.135
HV*LV*Toff	0.01046	0.00523	0.004904	1.07	0.294
HV*Ton*Toff	-0.00487	-0.00244	0.004904	-0.50	0.623
LV*Ton*Toff	-0.02704	-0.01352	0.004904	-2.76	0.010
HV*LV*Ton*Toff	-0.00271	-0.00135	0.004904	-0.28	0.784

S = 0.0339739 PRESS = 0.0831045
R-Sq = 35.60% R-Sq(pred) = 0.00% R-Sq(adj) = 5.41%

Analysis of Variance for R (coded units)

Source	DF	Seq SS	Adj SS	Adj MS	F	P
Main Effects	4	0.0010541	0.0010541	0.00026352	0.23	0.920
2-Way Interactions	6	0.0061888	0.0061888	0.00103147	0.89	0.511
3-Way Interactions	4	0.0130878	0.0130878	0.00327194	2.83	0.040
4-Way Interactions	1	0.0000880	0.0000880	0.00008802	0.08	0.784
Residual Error	32	0.0369353	0.0369353	0.00115423		
Pure Error	32	0.0369353	0.0369353	0.00115423		
Total	47	0.0573540				

Unusual Observations for R

Obs	StdOrder	R	Fit	SE Fit	Residual	St Resid
21	21	1.58300	1.52533	0.01961	0.05767	2.08R
36	36	1.61200	1.53567	0.01961	0.07633	2.75R

R denotes an observation with a large standardized residual.

Table XII. ANOVA Table of R for AISI-1045 considering all factors.

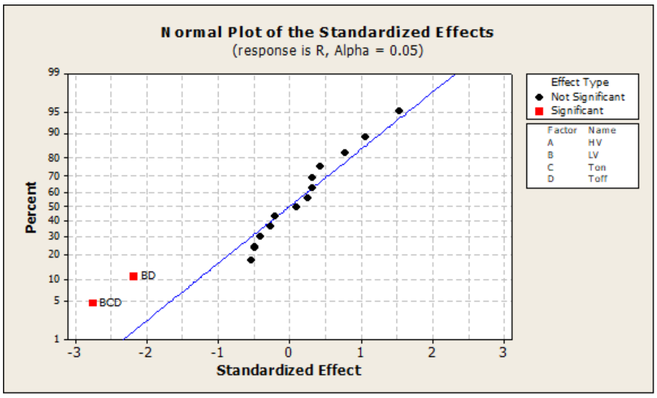

Figure XXXIV. Normal Probability Plot of the standardized effects of R for AISI-1045 considering all factors.

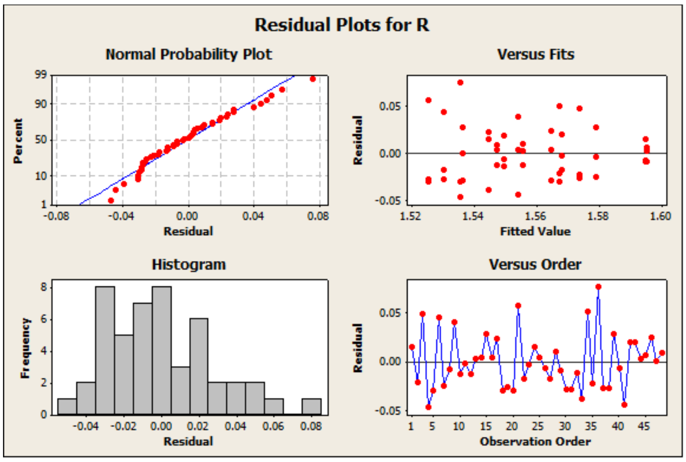

Figure XXXV. Residual Plot of R for AISI-1045 considering all factors.

Factorial Fit: R versus LV, Ton, Toff

Estimated Effects and Coefficients for R (coded units)

Term	Effect	Coef	SE Coef	T	P
Constant		1.55752	0.004577	340.30	0.000
LV	0.00754	0.00377	0.004577	0.82	0.415
Ton	0.00304	0.00152	0.004577	0.33	0.741
Toff	0.00246	0.00123	0.004577	0.27	0.790
LV*Toff	-0.02138	-0.01069	0.004577	-2.34	0.024
LV*Ton*Toff	-0.02704	-0.01352	0.004577	-2.95	0.005

S = 0.0317093   PRESS = 0.0551578

R-Sq = 26.37%   R-Sq(pred) = 3.83%   R-Sq(adj) = 17.60%

Analysis of Variance for R (coded units)

Source	DF	Seq SS	Adj SS	Adj MS	F	P
Main Effects	3	0.0008661	0.0008661	0.00028869	0.29	0.834
2-Way Interactions	1	0.0054827	0.0054827	0.00548269	5.45	0.024

3-Way Interactions	1	0.0087750	0.0087750	0.00877502	8.73	0.005
Residual Error	42	0.0422302	0.0422302	0.00100548		
Lack of Fit	2	0.0001220	0.0001220	0.00006102	0.06	0.944
Pure Error	40	0.0421082	0.0421082	0.00105270		
Total	47	0.0573540				

Unusual Observations for R

Obs	StdOrder	R	Fit	SE Fit	Residual	St Resid
3	3	1.62200	1.55571	0.01121	0.06629	2.23R
4	4	1.48900	1.55571	0.01121	-0.06671	-2.25R
34	34	1.61800	1.55383	0.01121	0.06417	2.16R

R denotes an observation with a large standardized residual.

* NOTE * Estimated regression coefficients in uncoded units are not available because the model is non-hierarchical.

Table XIII. ANOVA Table of R for AISI-1045 considering significant factors.

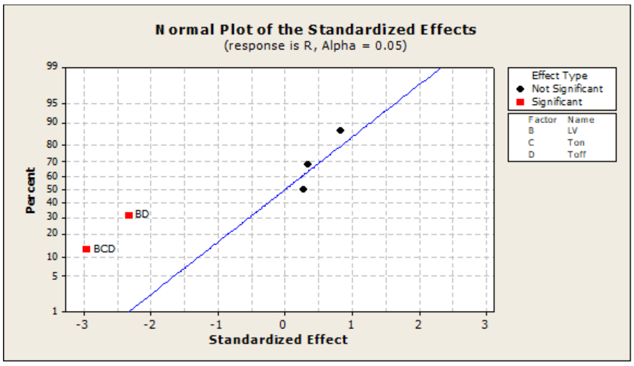

Figure XXXVI. Normal Probability Plot of the standardized effects of R for AISI-1045 considering significant factors.

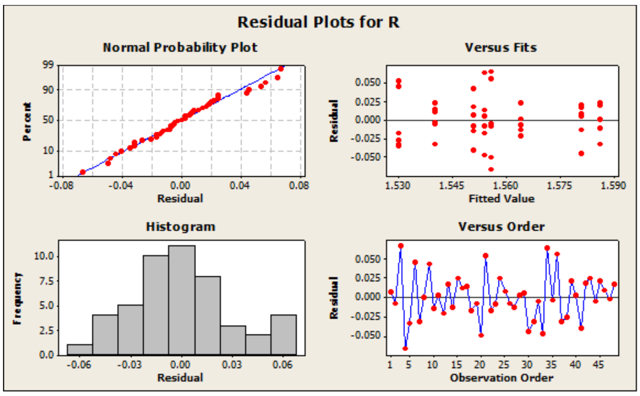

Figure XXXVII. Residual Plot of R for AISI-1045 considering all factors.

Memoria Investigaciones en Ingeniería, núm. 28 (2025). pp. 222-268
https://doi.org/10.36561/ING.28.15
ISSN 2301-1092 • ISSN (en línea) 2301-1106 – Universidad de Montevideo, Uruguay

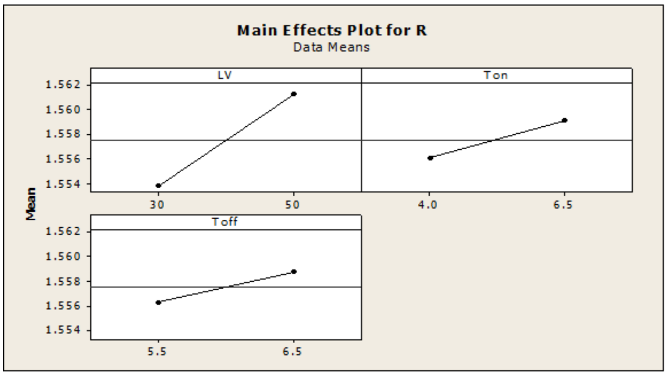

Figure XXXVIII. Main Effects Plot of R for AISI-1045 considering significant factors.

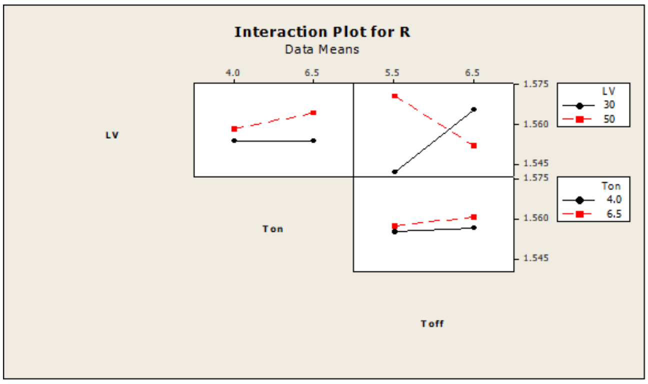

Figure XXXIX. Residual Plot of R for AISI-1045 considering Ton, Toff& LV.

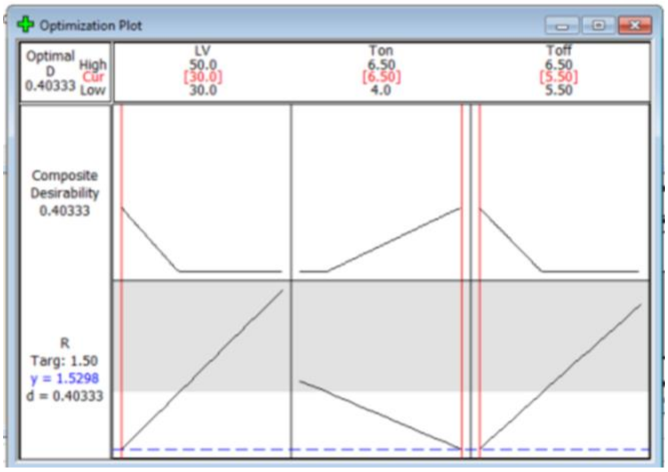

Figure XL. Optimization Plot of R for AISI-1045 for significant factors

Appendix 7

Run Order	HV	LV	T_{on}	T_{off}	Work Piece Material	E_a	W_a	Duty Factor %
1	0.3	30	4	5.5	AISI-1045	9.356	258.952	42%
2	0.7	30	4	5.5	AISI-1045	9.216	258.786	42%
3	0.3	50	4	5.5	AISI-1045	9.705	258.62	42%
4	0.7	50	4	5.5	AISI-1045	9.565	258.468	42%
5	0.3	30	6.5	5.5	AISI-1045	9.833	258.312	54%
6	0.7	30	6.5	5.5	AISI-1045	9.712	258.163	54%
7	0.3	50	6.5	5.5	AISI-1045	9.382	257.965	54%
8	0.7	50	6.5	5.5	AISI-1045	9.259	257.792	54%
9	0.3	30	4	6.5	AISI-1045	9.389	257.61	38%
10	0.7	30	4	6.5	AISI-1045	9.252	257.452	38%
11	0.3	50	4	6.5	AISI-1045	9.172	257.28	38%
12	0.7	50	4	6.5	AISI-1045	9.034	257.12	38%
13	0.3	30	6.5	6.5	AISI-1045	9.787	256.953	50%
14	0.7	30	6.5	6.5	AISI-1045	9.652	256.785	50%
15	0.3	50	6.5	6.5	AISI-1045	9.505	256.606	50%
16	0.7	50	6.5	6.5	AISI-1045	9.362	256.452	50%
17	0.3	30	4	5.5	AISI-1045	12.067	261.575	42%
18	0.7	30	4	5.5	AISI-1045	11.941	261.397	42%
19	0.3	50	4	5.5	AISI-1045	9.585	261.249	42%
20	0.7	50	4	5.5	AISI-1045	9.439	261.076	42%
21	0.3	30	6.5	5.5	AISI-1045	9.223	260.91	54%
22	0.7	30	6.5	5.5	AISI-1045	9.098	260.725	54%
23	0.3	50	6.5	5.5	AISI-1045	9.622	260.565	54%
24	0.7	50	6.5	5.5	AISI-1045	9.49	260.386	54%
25	0.3	30	4	6.5	AISI-1045	9.519	260.217	38%

26	0.7	30	4	6.5	AISI-1045	9.375	260.052	38%
27	0.3	50	4	6.5	AISI-1045	8.112	259.909	38%
28	0.7	50	4	6.5	AISI-1045	7.966	259.763	38%
29	0.3	30	6.5	6.5	AISI-1045	9.219	259.615	50%
30	0.7	30	6.5	6.5	AISI-1045	9.092	259.448	50%
31	0.3	50	6.5	6.5	AISI-1045	9.199	259.297	50%
32	0.7	50	6.5	6.5	AISI-1045	9.056	259.131	50%
33	0.3	30	4	5.5	AISI-1045	12.453	249.045	42%
34	0.7	30	4	5.5	AISI-1045	12.332	248.884	42%
35	0.3	50	4	5.5	AISI-1045	12.398	248.713	42%
36	0.7	50	4	5.5	AISI-1045	12.167	248.542	42%
37	0.3	30	6.5	5.5	AISI-1045	12.706	248.345	54%
38	0.7	30	6.5	5.5	AISI-1045	12.591	248.198	54%
39	0.3	50	6.5	5.5	AISI-1045	18.431	248.042	54%
40	0.7	50	6.5	5.5	AISI-1045	18.299	247.864	54%
41	0.3	30	4	6.5	AISI-1045	12.718	247.694	38%
42	0.7	30	4	6.5	AISI-1045	12.58	247.524	38%
43	0.3	50	4	6.5	AISI-1045	13.194	247.354	38%
44	0.7	50	4	6.5	AISI-1045	13.064	247.172	38%
45	0.3	30	6.5	6.5	AISI-1045	12.272	246.999	50%
46	0.7	30	6.5	6.5	AISI-1045	12.137	246.83	50%
47	0.3	50	6.5	6.5	AISI-1045	12.041	246.66	50%
48	0.7	50	6.5	6.5	AISI-1045	11.905	246.506	50%

Table XIV. Experimental inputs for AISI-1045 material with three replicates.

Appendix 8

Run Order	Tm (sec)	MRR (g/min)	EW (g/min)	Base Radius (mm)	Surface Roughness (R_a) (mm)
1	1094	0.0091	0.00768	1.56	0.042
2	1149	0.00867	0.00674	1.546	0.012
3	1034	0.00882	0.00812	1.622	0.014
4	668	0.01401	0.01105	1.489	0.04
5	602	0.01485	0.01126	1.495	0.013
6	779	0.01525	0.00986	1.575	0.038
7	505	0.02055	0.01461	1.554	0.042
8	343	0.03184	0.01977	1.586	0.033
9	495	0.01915	0.01661	1.594	0.026
10	729	0.01416	0.01111	1.536	0.057
11	1021	0.0094	0.00811	1.566	0.029
12	1124	0.00891	0.00817	1.543	0.052
13	822	0.01226	0.00985	1.598	0.02
14	867	0.01239	0.00941	1.568	0.043
15	720	0.01283	0.01192	1.564	0.038
16	694	0.01418	0.01141	1.551	0.023
17	957	0.01116	0.0079	1.568	0.23
18	1055	0.00842	0.00671	1.537	0.011
19	800	0.01298	0.01095	1.548	0.056
20	822	0.01212	0.00869	1.506	0.017
21	517	0.02147	0.01451	1.583	0.018
22	506	0.01897	0.01494	1.513	0.028
23	719	0.01494	0.01102	1.576	0.031
24	793	0.01279	0.00968	1.61	0.111
25	904	0.01095	0.00956	1.558	0.024
26	745	0.01152	0.00999	1.543	0.069
27	943	0.00929	0.00929	1.55	0.027
28	1069	0.00831	0.00769	1.566	0.03
29	772	0.01298	0.00987	1.586	0.05
30	813	0.01114	0.00989	1.536	0.033
31	789	0.01262	0.01087	1.508	0.036
32	478	0.02247	0.01607	1.535	0.025
33	1173	0.00824	0.00619	1.506	0.023
34	1248	0.00822	0.00644	1.618	0.013
35	1036	0.0099	0.01338	1.551	0.019
36	1231	0.0096	0.00551	1.612	0.019
37	948	0.0093	0.00728	1.498	0.018
38	872	0.01073	0.00853	1.503	0.054
39	490	0.0218	0.01616	1.607	0.01

40	702	0.01453	0.01128	1.588	0.021
41	1066	0.00957	0.00777	1.51	0.014
42	1007	0.01013	0.00739	1.569	0.026
43	874	0.01249	0.00892	1.588	0.026
44	1182	0.00878	0.00726	1.558	0.032
45	976	0.01039	0.0083	1.601	0.018
46	928	0.01099	0.00873	1.589	0.051
47	756	0.01222	0.01071	1.537	0.043
48	772	0.01298	0.01111	1.556	0.069

Table XV. Experimental Responses for AISI-1045along with three Replicates.

Appendix 9. - The AISI-1045 workpiece surface outline images were taken at a magnification level of 22X

Experimental Runs	**Replicate # 1**	**Replicate # 2**	**Replicate # 3**
1			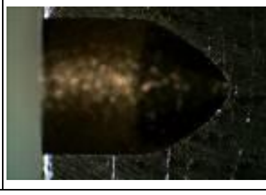
T_{on} = 4µs,T_{off}5.5 µs,Duty Factor = 42%, HV = 0.3V, LV = 30A			
2		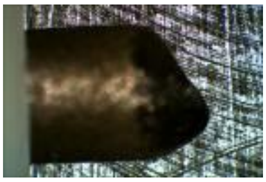	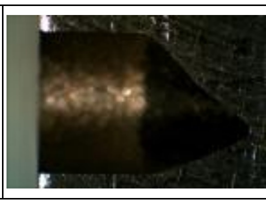
T_{on} = 4µs,T_{off}5.5 µs,Duty Factor = 42%, HV = 0.7V, LV = 30A			
3			
T_{on} = 4µs,T_{off}5.5 µs,Duty Factor = 42%, HV = 0.3V, LV = 50A			
4		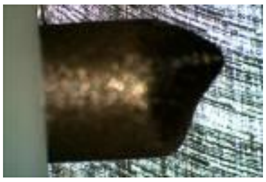	
T_{on} = 4µs,T_{off}5.5 µs,Duty Factor = 42%, HV = 0.7V, LV = 50A			
5			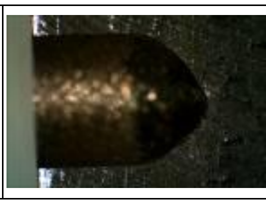
T_{on} = 6.5µs,T_{off}5.5 µs,Duty Factor = 54%, HV = 0.3V, LV = 30A			
6		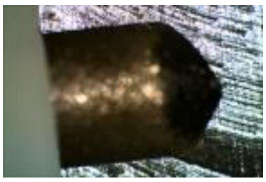	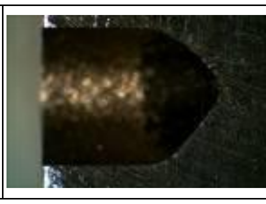
T_{on} = 6.5µs,T_{off}5.5 µs,Duty Factor = 54%, HV = 0.7V, LV = 30A			
7			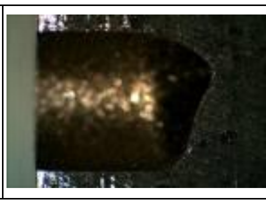

Experimental Runs	**Replicate # 1**	**Replicate # 2**	**Replicate # 3**
T_{on} = 6.5µs,T_{off}5.5 µs,Duty Factor = 54%, HV = 0.3V, LV = 50A			
8			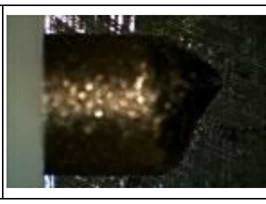
T_{on} = 6.5µs,T_{off}5.5 µs,Duty Factor = 54%, HV = 0.7V, LV = 50A			
9			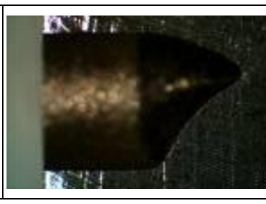
T_{on} = 4µs,T_{off}6.5 µs,Duty Factor = 38%, HV = 0.3V, LV = 30A			
10	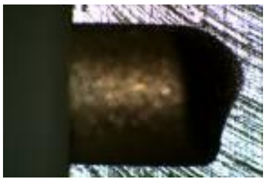		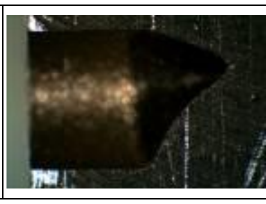
T_{on} = 4µs,T_{off}6.5 µs,Duty Factor = 38%, HV = 0.7V, LV = 30A			
11	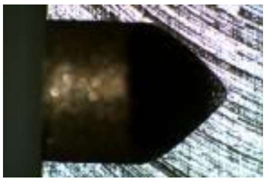	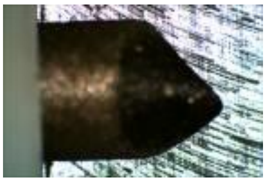	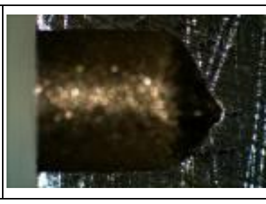
T_{on} = 4µs,T_{off}6.5 µs,Duty Factor = 38%, HV = 0.3V, LV = 50A			
12	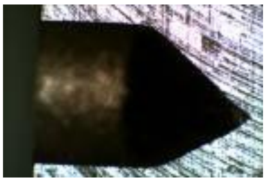	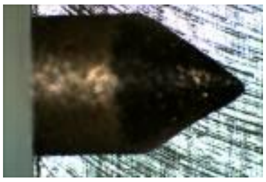	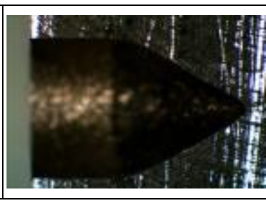
T_{on} = 4µs,T_{off}6.5 µs,Duty Factor = 38%, HV = 0.7V, LV = 50A			
13		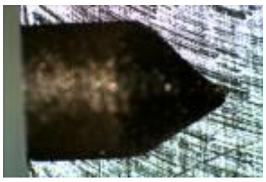	
T_{on} = 6.5µs,T_{off}6.5 µs,Duty Factor = 50%, HV = 0.3V, LV = 30A			
14	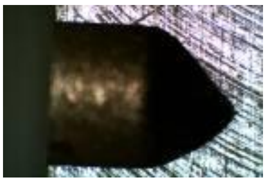		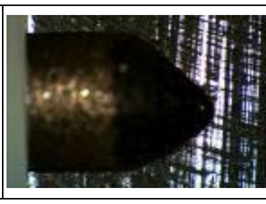
T_{on} = 6.5µs,T_{off}6.5 µs,Duty Factor = 50%, HV = 0.7V, LV = 30A			

Experimental Runs	**Replicate # 1**	**Replicate # 2**	**Replicate # 3**
15		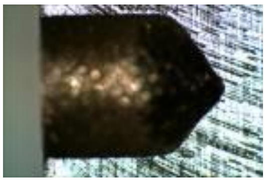	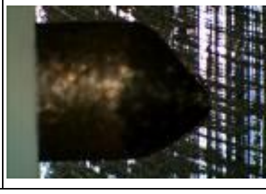
$T_{on\,=}$ 6.5µs,T_{off}6.5 µs,Duty Factor = 50%, HV = 0.3V, LV = 50A			
16			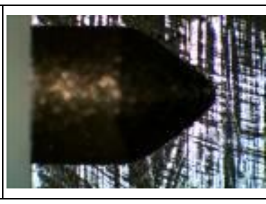
$T_{on\,=}$ 6.5µs,T_{off}6.5 µs,Duty Factor = 50%, HV = 0.7V, LV = 50A			

Table XVI. AISI 1045 Workpiece Outline 22X.

Appendix 10. - The electrode images that machined AISI-1045 were taken at a magnification level of 20 X

Experimental Runs	**Replicate # 1**	**Replicate # 2**	**Replicate # 3**
1			
T_{on} = 4µs, T_{off} 5.5 µs, Duty Factor = 42%, HV = 0.3, LV = 30			
2		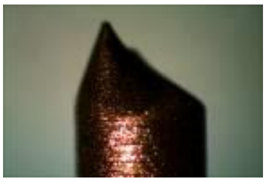	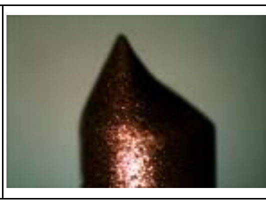
T_{on} = 4µs, T_{off} 5.5 µs, Duty Factor = 42%, HV = 0.7, LV = 30			
3			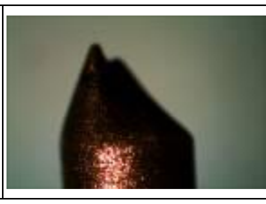
T_{on} = 4µs, T_{off} 5.5 µs, Duty Factor = 42%, HV = 0.3, LV = 50			
4	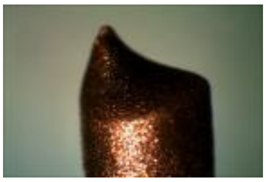		
T_{on} = 4µs, T_{off} 5.5 µs, Duty Factor = 42%, HV = 0.7, LV = 50			
5			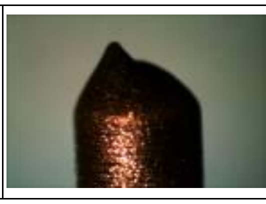
T_{on} = 6.5µs, T_{off} 5.5 µs, Duty Factor = 54%, HV = 0.3, LV = 30			
6			
T_{on} = 6.5µs, T_{off} 5.5 µs, Duty Factor = 54%, HV = 0.7, LV = 30			
7	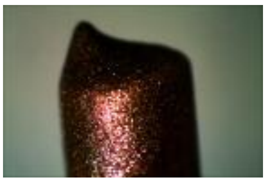		
T_{on} = 6.5µs, T_{off} 5.5 µs, Duty Factor = 54%, HV = 0.3, LV = 50			

https://doi.org/10.36561/ING.28.15
ISSN 2301-1092 • ISSN (en línea) 2301-1106 – Universidad de Montevideo, Uruguay

Experimental Runs	**Replicate # 1**	**Replicate # 2**	**Replicate # 3**
8			
T_{on} = 6.5µs,T_{off}5.5 µs,Duty Factor = 54%, HV = 0.7, LV = 50			
9			
T_{on} = 4µs,T_{off}6.5 µs,Duty Factor = 38%, HV = 0.3, LV = 30			
10			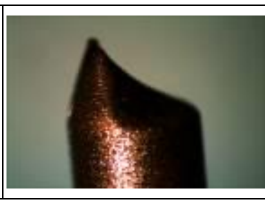
T_{on} = 4µs,T_{off}6.5 µs,Duty Factor = 38%, HV = 0.7, LV = 30			
11			
T_{on} = 4µs,T_{off}6.5 µs,Duty Factor = 38%, HV = 0.3, LV = 50			
12			
T_{on} = 4µs,T_{off}6.5 µs,Duty Factor = 38%, HV = 0.7, LV = 50			
13			
T_{on} = 6.5µs,T_{off}6.5 µs,Duty Factor = 50%, HV = 0.3, LV = 30			
14			
T_{on} = 6.5µs,T_{off}6.5 µs,Duty Factor = 50%, HV = 0.7, LV = 30			

Experimental Runs	**Replicate # 1**	**Replicate # 2**	**Replicate # 3**
15			
$T_{on =}$ 6.5µs,T_{off}6.5 µs,Duty Factor = 50%, HV = 0.3, LV = 50			
16			
$T_{on =}$ 6.5µs,T_{off}6.5 µs,Duty Factor = 50%, HV = 0.7, LV = 50			

Table XVII. AISI 1045– Copper Electrode – 20 X.

Author contribution:
1. Conception and design of the study
2. Data acquisition
3. Data analysis
4. Discussion of the results
5. Writing of the manuscript
6. Approval of the last version of the manuscript

MMUZS has contributed to: 1, 2, 3, 4, 5 and 6.
SAI has contributed to: 1, 2, 3, 4, 5 and 6.
AZ has contributed to: 1, 2, 3, 4, 5 and 6.
AT has contributed to: 1, 2, 3, 4, 5 and 6.

Acceptance Note: This article was approved by the journal editors Dr. Rafael Sotelo and Mag. Ing. Fernando A. Hernández Gobertti.